© 2015. Published by The Company of Biologists Ltd | Development (2015) 142, 331-342 doi:10.1242/dev.118422

RESEARCH ARTICLE

Enteric neural crest cells regulate vertebrate stomach patterning and differentiation

Sandrine Faure*, Jennifer McKey, Sébastien Sagnol and Pascal de Santa Barbara*

ABSTRACT

In vertebrates, the digestive tract develops from a uniform structure where reciprocal epithelial-mesenchymal interactions pattern this complex organ into regions with specific morphologies and functions. Concomitant with these early patterning events, the primitive GI tract is colonized by the vagal enteric neural crest cells (vENCCs), a population of cells that will give rise to the enteric nervous system (ENS), the intrinsic innervation of the GI tract. The influence of vENCCs on early patterning and differentiation of the GI tract has never been evaluated. In this study, we report that a crucial number of vENCCs is required for proper chick stomach development, patterning and differentiation. We show that reducing the number of vENCCs by performing vENCC ablations induces sustained activation of the BMP and Notch pathways in the stomach mesenchyme and impairs smooth muscle development. A reduction in vENCCs also leads to the transdifferentiation of the stomach into a stomach-intestinal mixed phenotype. In addition, sustained Notch signaling activity in the stomach mesenchyme phenocopies the defects observed in vENCC-ablated stomachs, indicating that inhibition of the Notch signaling pathway is essential for stomach patterning and differentiation. Finally, we report that a crucial number of vENCCs is also required for maintenance of stomach identity and differentiation through inhibition of the Notch signaling pathway. Altogether, our data reveal that, through the regulation of mesenchyme identity, vENCCs act as a new mediator in the mesenchymal-epithelial interactions that control stomach development.

KEY WORDS: Gut development, Smooth muscle differentiation, Enteric neural crest cells, Notch pathway, Mesenchymal-epithelial interactions, Chick

INTRODUCTION

The vertebrate gastrointestinal (GI) tract is a remarkably complex organ system that originates from the three embryonic germ layers: endoderm (which forms the epithelial lining of the lumen), mesoderm (which forms the smooth muscle layers and the network of interstitial cells of Cajal) and ectoderm (which includes the most posterior luminal digestive structure and the enteric nervous system network). The primitive GI tract consists initially of a straight and uniform tube of epithelium surrounded by mesenchyme. Reciprocal epithelial-mesenchymal interactions drive the development and regionalization of the GI tract and maintain its regionalized architecture until adulthood (de Santa Barbara et al., 2002; Faure and de Santa Barbara, 2011). Sonic hedgehog (SHH) signals from the GI epithelium to the adjacent mesenchyme and induces region-restricted expression of genes, such as homeotic genes (*Hox*, *Nkx*) and *Bmp4*, a member of the bone morphogenetic protein (BMP) pathway (Roberts et al., 1995, 1998; Buchberger et al., 1996; Smith and Tabin, 1999; Smith et al., 2000). The mesenchyme in turn signals back to the epithelium to control its patterning and differentiation along the anteroposterior (AP) axis (Kedinger et al., 1986, 1990; Roberts et al., 1998; de Santa Barbara et al., 2002, 2003).

Such molecular mechanisms are also required later during development when the mesenchyme of the whole GI tract differentiates along the radial axis and gives rise (from the outer to the inner part of the gut wall) to the longitudinal and circular muscle layers, the submucosae, and the muscularis mucosae close to the epithelial lining (Ramalho-Santos et al., 2000; Sukegawa et al., 2000; de Santa Barbara et al., 2005; Kosinski et al., 2010; Mao et al., 2010). Differentiation of digestive mesenchymal cells into smooth muscle cells (SMCs) can be characterized first through their elongation and clustering and later by the expression of SMC-specific lineage markers, such as α 1 smooth muscle actin (αSMA), smooth muscle protein 22 (SM22) and calponin, which precedes smooth muscle cell contractile functions (Gabella, 2002).

Concomitant with these early patterning events, the primitive GI tract is colonized by neural crest precursors, a population of cells that give rise to the enteric nervous system (ENS), which forms the intrinsic innervation of the GI tract. In chick, the ENS is predominantly derived from vagal enteric neural crest cells (vENCCs) that migrate from the neural tube adjacent to somites 1 to 7 (Yntema and Hammond, 1954; Le Douarin and Teillet, 1973; Burns and Le Douarin, 1998; Burns et al., 2000). These cells exit the neural tube, enter the esophagal mesenchyme and begin an anterior to posterior wave of migration through their interaction with mesenchymal extracellular matrix proteins (Fairman et al., 1995; Burns and Le Douarin, 1998). This allows vENCCs to populate the entire GI tract, from the esophagus to the terminal colon. As the neural crest cells migrate along the GI tract, they proliferate and finally differentiate into neurons and glial cells of the ENS, and form two concentric plexuses of ganglion cells localized in muscle layers of the gut wall (Furness, 2006).

However, despite their well-known innervative function in adult GI tract, the contribution of the ENS network to the development and differentiation of the GI tract has never been addressed. Here, we show that a crucial number of vENCCs is required for proper chick stomach development. Our findings suggest an unexpected new function of vENCCs in regulating both the establishment and the maintenance of stomach patterning and differentiation through inhibition of the Notch signaling pathway.

RESULTS

A crucial number of vENCCs is necessary for stomach smooth muscle differentiation

Using the chick embryo as a model organism, we first examined and compared the kinetics of vENCC migration and the differentiation of

INSERM U1046, Université Montpellier 1, Université Montpellier 2, Montpellier 34295, France.

*Authors for correspondence (sandrine.faure@inserm.fr; pascal.de-santa-barbara@inserm.fr)

Received 3 October 2014; Accepted 25 November 2014

Development (2015) 142, 331-342 doi:10.1242/dev.118422

mesenchymal cells into smooth muscle cells, by immunofluorescence analysis using anti-HNK-1 (marker of neural crest cells) and anti-αSMA (marker of determined SMCs) antibodies (Tucker et al., 1984; Gabella, 2002) (Fig. 1). At E4 (HH23), vENCCs were randomly distributed in the mesenchyme of the developing stomach and duodenum. Conversely, no αSMA-positive cells were detected in E4 stomachs, indicating that the mesenchyme had not yet began to be specified (Fig. 1A, white arrow). As a positive control, we detected αSMA-expressing cells in blood vessels associated with the intestine (Fig. 1A, red arrow). In E5-E5.5 (HH27) stomachs, we began to detect αSMA-positive cells in the mesenchyme and vENCCs were more abundant and organized (Fig. 1B,C). At E7.5 (HH32), the stomach mesenchyme was then fully organized into smooth muscle and submucosal layers and vENCCs were localized in enteric ganglia located at the periphery of the smooth muscle domain (Fig. 1D,E).

The observation that stomach smooth muscle specification is initiated after its colonization by vENCCs (Fig. 1A) prompted us to investigate the influence of vENCCs on stomach mesenchyme development. To this aim, we surgically reduced the number of vENCCs that colonize the GI tract, by ablating the dorsal neural tube adjacent to somites 3 to 6 in E1.5 (HH10) chicken embryos, as previously described (Peters-van der Sanden et al., 1993; Burns et al., 2000; Barlow et al., 2008) (supplementary material Fig. S1A). Control and vENCC-ablated GI tracts were then dissected and analyzed at E7.5, when mesenchymal cells have differentiated into smooth muscle cells. The global morphology of whole vENCC-ablated embryos was indistinguishable from control embryos, demonstrating the absence of growth alterations induced by the micromanipulation (supplementary material Fig. S1B). Visual inspection of GI morphology revealed shrunken and malformed stomachs, whereas the intestine appeared normal in GI tracts from vENCC-ablated embryos compared with controls (Fig. 2A, n=84/120). Moreover, the rostral part of the stomach (proventriculus) was often centralized in stomachs from vENCC-ablated embryos compared with controls (Fig. 2A, white arrowhead, n=72/120). Immunostaining analysis of paraffin-embedded stomach sections using the anti-HNK-1 antibody indicated that ENS development was abnormal in stomachs from vENCC-ablated embryos (which we will refer as vENCC-ablated stomachs) compared with the controls. In the representative experiment shown in Fig. 2B, vENCCs were reduced by 60.55% and the network of the remaining vENCCs was less organized than in controls (absence of enteric ganglia and increased number of isolated HNK-1-positive cells) (Fig. 2B-D). We next evaluated the effect of vENCC ablation on the mesenchyme, by performing immunofluorescence staining on paraffin-embedded stomach sections and reverse-transcription quantitative polymerase chain reaction (RT-qPCR) analyses of whole stomachs. These experiments showed that smooth muscle development was hindered in vENCC-ablated stomachs compared with controls, as indicated by the reduction in the expression of smooth muscle markers (αSMA, calponin and *Sm22*) and myocardin, a serum response factor (SRF) co-activator that controls many steps of smooth muscle differentiation (Fig. 2E,F). These results are in line with a contribution of vENCCs to stomach smooth muscle development.

A crucial number of vENCCs is necessary for proper stomach patterning

Our results (Fig. 2A) also suggest a role for the vENCCs during stomach development. We found that vENCC-ablated stomachs were histologically characterized by a thinner mesenchymal layer compared with the controls (Fig. 3A). This could result either from an increase in mesenchymal cell death or a decrease in mesenchymal cell proliferation, or both. To address this question, we performed immunostaining for cleaved caspase 3, a standard marker of cell death (Mao et al., 2010) and phosphorylated histone 3-Ser10 (PH3), a standard marker of G2/M transition (Notarnicola et al., 2012). Although we did not detect a significant change in the

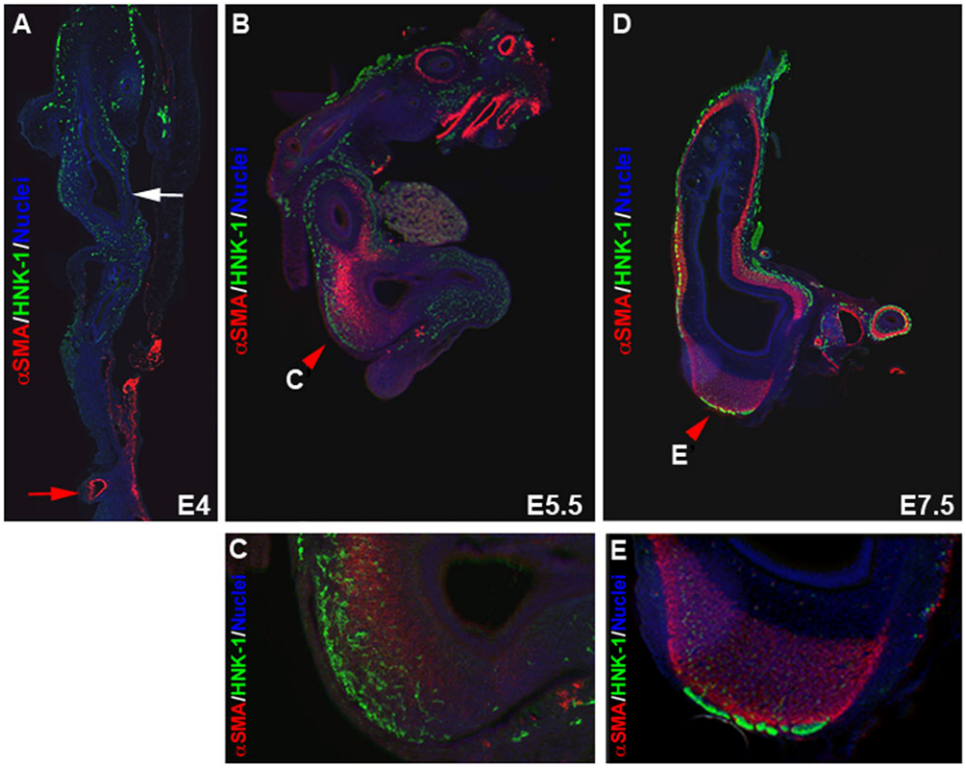

Fig. 1. Stomach smooth muscle differentiation is initiated after vENCC colonization. (A-E) Immunostaining analysis of paraffin-embedded stomach tissues using anti-αSMA (red; SMC marker) and anti-HNK-1 (green; ENCC marker) antibodies. Nuclei were stained with Hoechst (blue). Longitudinal stomach sections at E4 (A), E5.5 (B) and E7.5 (D). The white arrow in A indicates the absence of αSMA-positive cells in the mesenchyme of the stomach. The red arrow in A indicates the αSMA-positive blood vessel. (C,E) Magnified views of the domains indicated by red arrowheads in B and D.

Development (2015) 142, 331-342 doi:10.1242/dev.118422

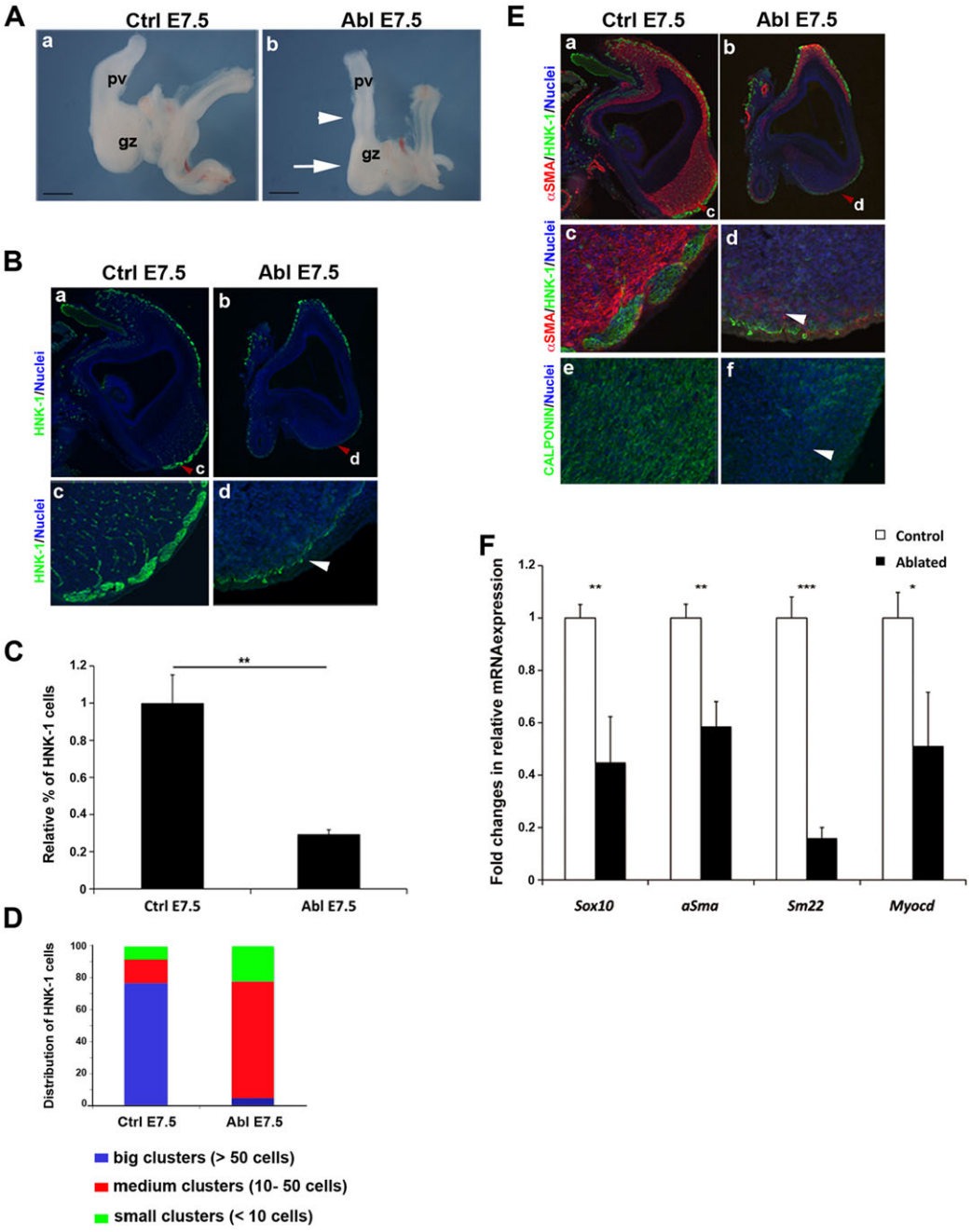

Fig. 2. A crucial number of vENCCs is necessary for stomach smooth muscle development. vENCCs were ablated by microsurgically removing the dorsal part of the neural tube between somites 3 and 6 in HH10 (E1.5) chick embryos. Control guts and guts from vENCC-ablated embryos were dissected at E7.5. (A) Phenotypes of whole guts. Representative example of guts from control (Ctrl E7.5) (a) and vENCC-ablated embryos (Abl E7.5) (b). The stomach of the vENCC-ablated embryo is much smaller (white arrow) and the proventriculus (white arrowhead) is centralized compared with the control. pv, proventriculus; gz, gizzard. Scale bars: 1 mm. (B) Immunostaining analysis of paraffin-embedded sections using an anti-HNK-1 antibody (green) to specifically detect vENCCs and evaluate the efficiency of ablation. Nuclei were stained with Hoechst (blue). (a,c) Control stomach (Ctrl E7.5) and (b,d) stomach from a vENCC-ablated embryo (Abl E7.5). c and d are magnified views of the regions indicated by red arrowheads in a and b. The white arrowhead in d shows that the enteric nervous system is abnormal in the stomach of vENCC-ablated embryos compared with the control. (C) Quantification of HNK-1-positive cells (from B) in stomachs from control (Ctrl E7.5) and vENCC-ablated embryos (Abl E7.5). This was accomplished by counting the number of HNK-1-positive cells relative to the total number of cells. Five different regions per section were analyzed on five sections per slide. Four slides were processed for each condition. Our results show that HNK-1-positive cells were reduced by 60.55% in the gizzard mesenchyme of vENCC-ablated embryos compared with controls. $^{**}P<0.01$. Student's *t*-test. Error bars indicate s.e.m. (D) Analysis of the distribution of HNK-1-positive cells in the mesenchyme of stomachs from control (Ctrl E7.5) and vENCC-ablated embryos (Abl E7.5). The remaining HNK-1-positive cells in stomachs from vENCC-ablated embryos form a less organized network than in controls, and they are mainly organized in medium clusters (10 to 50 cells per cluster). (E) Immunostaining analysis of paraffin-embedded stomach sections from (a,c,e) control (Ctrl E7.5) and (b,d,f) vENCC-ablated embryos (Abl E7.5) using anti-αSMA (red; SMC marker) and anti-HNK-1 (green; ENCC marker) or anti-calponin (green) antibodies. Nuclei were labeled with Hoechst (blue); c and d are magnified views of the regions indicated by red arrowheads in a and b. A reduced number of vENCCs strongly impairs smooth muscle development, as indicated by the strong reduction in αSMA (white arrowhead d) and calponin (white arrowhead in f) staining in vENCC-ablated stomach compared with the control. (F) Quantification of gene expression by RT-qPCR in E7.5 stomachs from control (Control) and vENCC-ablated embryos (Ablated). Normalized expression levels were converted to fold changes. $^{**}P<0.01$ or $^{***}P<0.001$. Error bars indicate s.e.m.

Development (2015) 142, 331-342 doi:10.1242/dev.118422

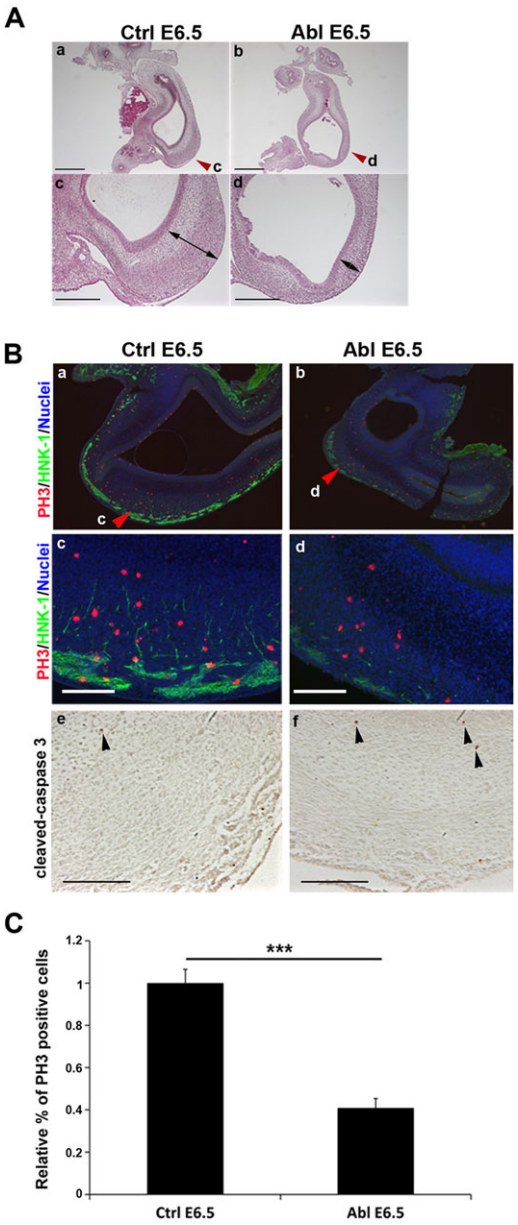

Fig. 3. Detailed analysis of morphological defects observed in vENCC-ablated stomachs. vENCCs were ablated by microsurgically removing the dorsal part of the neural tube between somites 3 and 6 from HH10 chick embryos and dissected at stage E6.5. (A) Hematoxylin and Eosin staining of paraffin-embedded stomach sections from (a,c) control (Ctrl E6.5) and (b,d) vENCC-ablated embryos (Abl E6.5). c and d are magnified views of the regions highlighted by red arrowheads in a and b. Scale bars: 500 µm in a,b; 250 µm in c,d. (B) Paraffin-embedded stomach sections from (a,c,e) controls (Ctrl E6.5) and (b,d,f) vENCC-ablated embryos (Abl E6.5) were analyzed by immunofluorescence (a-d) using anti-PH3 (red; G2/M transition marker) and anti-HNK-1 (green; vENCC marker) antibodies. Nuclei were labeled with Hoechst (blue). c and d are magnified views of the regions indicated by red arrowheads in a and b. Scale bars: 100 µm. Immunohistochemistry analysis performed on serial sections using the anti-cleaved caspase 3 antibody (e,f) that specifically detects apoptotic cells. Black arrowheads indicate cleaved caspase 3-positive apoptotic cells. (C) Quantification of PH3-positive cells in stomachs dissected from control (Ctrl E6.5) or vENCC-ablated embryos (Abl E6.5). Proliferation rates were assessed by counting the number of PH3-positive cells relative to the total number of nuclei in the section. Three control stomachs and three stomach dissected from vENCC-ablated embryos were processed. Six slides for each stomach were analyzed. ***P<0.001. Student's t-test. Error bars indicate s.e.m.

number of cleaved caspase 3-positive cells, we found that the rate of cell proliferation was statistically decreased by 59.1% in the mesenchyme of vENCC-ablated stomachs compared with controls (Fig. 3B,C). We then examined the expression of genes involved in GI tract development and patterning. Compared with controls, vENCC-ablated stomachs did not show any change in *Barx1* expression (Fig. 4A,C), a specific marker of stomach mesenchyme (Barlow et al., 1999; Kim et al., 2005; supplementary material Fig. S2), suggesting that vENCC-ablated stomachs retained stomach properties. Conversely, *Bapx1*, a marker of stomach mesenchyme downstream of *Barx1* (Verzi et al., 2009; Faure et al., 2013; supplementary material Fig. S2), was strongly downregulated (Fig. 4A,C). *Bapx1* negatively regulates *Bmp4*, which is normally expressed in the whole GI mesenchyme, except for the gizzard (supplementary material Fig. S2) (Nielsen et al., 2001; de Santa Barbara et al., 2005). In addition, *Bmp4* has been shown to inhibit cell proliferation in the intestinal mesenchyme (Smith et al., 2000). Here, we observed that *Bmp4* was strongly upregulated in vENCC-ablated stomachs. This could contribute to the decrease in the rate of cell proliferation observed in mesenchyme of vENCC-ablated stomachs. Interestingly, the expression of the intestinal mesenchyme markers *Nkx2.3* and *Lef1* (Buchberger et al., 1996; Theodosiou and Tabin, 2003; supplementary material Fig. S2) was also observed in vENCC-ablated stomachs, suggesting that their mesenchyme harbors intestinal features (Fig. 4A,C). As it has been shown that instructive mesenchymal-epithelial interactions are at the basis of GI development and region-specific epithelial differentiation (Roberts, 2000; de Santa Barbara et al., 2003), we next investigated whether the adjacent epithelium could be affected following the transition from stomach mesenchyme to the mixed stomach/intestine phenotype. Although cytodifferentiation and integrity of the stomach epithelium were not affected in vENCC-ablated stomachs, as demonstrated by normal endodermal *Shh* expression (Fig. 4B), the molecular identity of the epithelium was altered. Specifically, SOX9, an intestinal epithelial marker (Moniot et al., 2004; Blache et al., 2004), was ectopically expressed in the stomach epithelium of E6.5 vENCC-ablated stomachs (Fig. 4B). Similarly, RT-qPCR analysis showed that expression of *CdxA*, a homeotic gene essential for intestinal epithelium identity (Lorentz et al., 1997; Silberg et al., 2000), was also detected in stomachs of vENCC-ablated stomachs (Fig. 4C). Thus, our results show that the mesenchymal and epithelial layers of stomachs from vENCC-ablated stomachs acquired intestinal features, suggesting that a crucial number of vENCCs is required for proper stomach patterning.

Inhibition of Notch signaling is required for stomach patterning and differentiation

This unexpected influence of vENCCs on stomach mesenchyme could be in part mediated by signaling pathways that control different aspects of development. As *Bmp4* expression was upregulated in stomachs from vENCC-ablated stomachs (Fig. 4A,C) and because a reduction in BMP activity is necessary for stomach patterning (Smith et al., 2000; Moniot et al., 2004; de Santa Barbara et al., 2005), we next used the avian replication-competent retroviral misexpression system to maintain BMP pathway activity in the developing stomach mesenchyme (Smith et al., 2000; Moniot et al., 2004; de Santa Barbara et al., 2005). Trophism of avian retroviruses is specific to mesenchymal cells and does not directly target ENCCs (Notarnicola et al., 2012; supplementary material Fig. S3). Maintaining BMP pathway activity by misexpressing *Bmp4* in the stomach mesenchyme inhibited smooth muscle development and

Development (2015) 142, 331-342 doi:10.1242/dev.118422

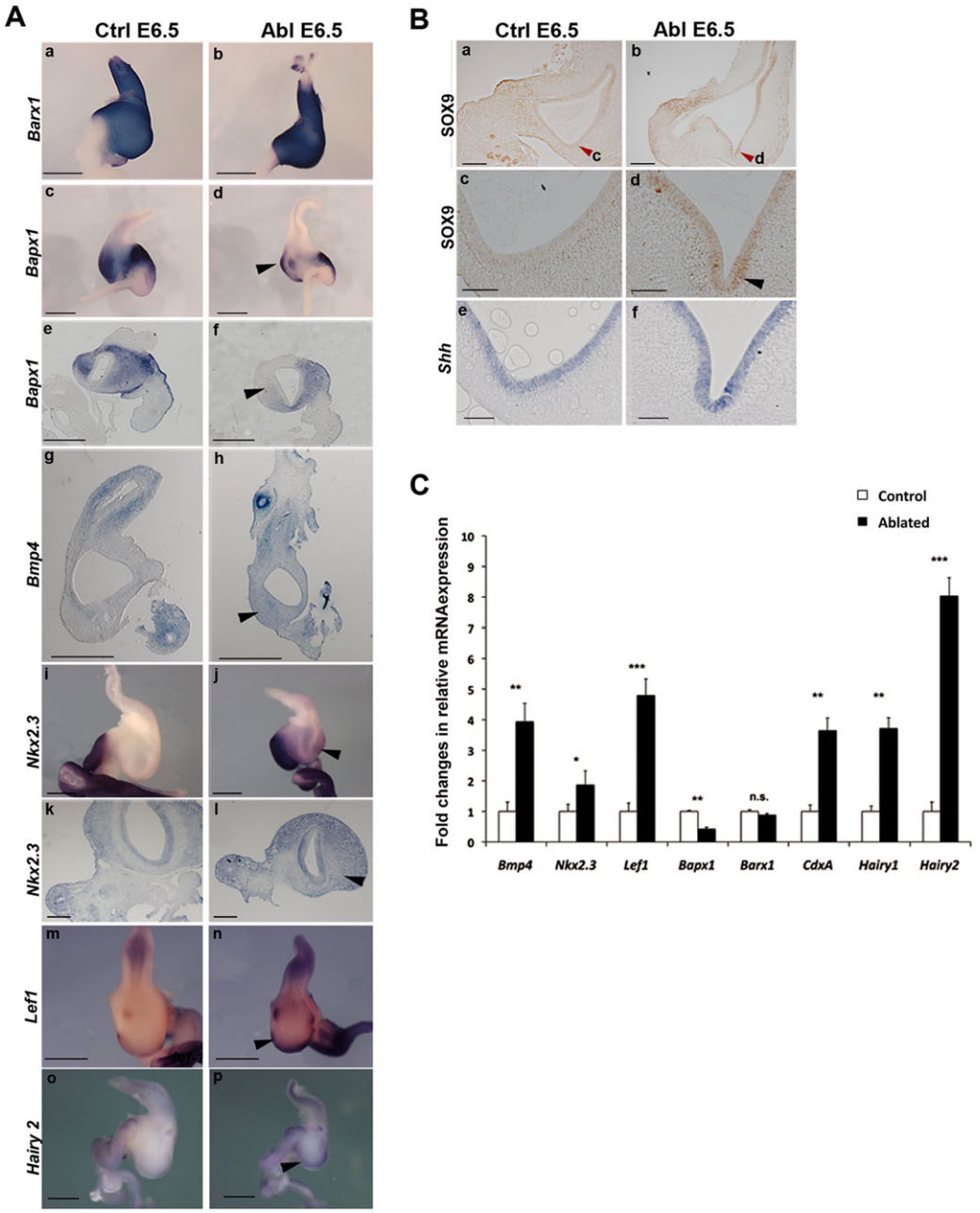

Fig. 4. A crucial number of vENCCs is necessary for stomach patterning. vENCCs were ablated by microsurgically removing the dorsal part of the neural tube between somites 3 and 6 from HH10 chick embryos. Control guts and guts from vENCC-ablated embryos were dissected at stage E6.5. (A) *In situ* hybridization of stomachs from control (Ctrl E6.5) (a,c,e,g,i,k,m,o) and vENCC-ablated (Abl E6.5) (b,d,f,h,j,l,n,p) guts. Whole-mount *in situ* hybridization using the *Barx1* (a,b) and *Bapx1* (c,d) probes. The black arrowhead in d indicates the low level of *Bapx1* expression in vENCC-ablated stomachs compared with control. Scale bars: 1 mm. *In situ* hybridization of paraffin-embedded sections using the *Bapx1* (e,f) and *Bmp4* (g,h) probes. The black arrowhead in f indicates the decrease in *Bapx1* expression in vENCC-ablated stomachs. The black arrowhead in h indicates the higher level of *Bmp4* expression in vENCC-ablated stomachs compared with control. Scale bars: 500 µm. *In situ* hybridization of whole stomachs (i,j) and of paraffin-embedded stomach sections (k,l) using the *Nkx2.3* probe. The black arrowheads in j and l demonstrate the increase in *Nkx2.3* expression in vENCC-ablated stomachs. Scale bars: 1 mm. Whole-mount *in situ* hybridization using *Lef1* (m,n) and *Hairy2* (o,p) probes. The black arrowheads in n and p show the increase in, respectively, *Lef1* and *Hairy2* expression in vENCC-ablated stomachs. Scale bars: 1 mm. (B) Anti-SOX9 immunohistochemistry analysis of stomach sections from (a,c) control (Ctrl E6.5) and (b,d) vENCC-ablated embryos. c and d are magnified views of the areas indicated by red arrowheads in a and b. Scale bars: 1 mm in a,b;. 100 µm in c,d. Black arrowhead in d shows SOX9 ectopic expression in the stomach epithelium of vENCC-ablated embryos compared with controls. (e,f) *In situ* hybridization analysis of paraffin-embedded stomach sections from control (e, Ctrl E6.5) and vENCC-ablated (f, Abl E6.5) embryos using the *Shh* probe indicates that Shh expression is comparable in stomach epithelium. Scale bars: 500 µm. (C) Quantification of gene expression by RT-qPCR in stomachs from control (Control) and vENCC-ablated embryos (Ablated). Normalized expression levels were converted to fold changes. $^{**}P<0.01$, $^{***}P<0.001$, n.s., not significant. Error bars indicate s.e.m.

induced pyloric mesenchyme features highlighted by the expression of *Nkx2.5* (Smith and Tabin, 1999). However, this failed to induce *Nkx2.3* ectopic expression in the targeted stomach (supplementary material Fig. S4), suggesting that BMP pathway activation in the mesenchyme of the stomach is not sufficient to gain intestinal properties. We next focused on the Notch pathway as it has been

Development (2015) 142, 331-342 doi:10.1242/dev.118422

reported that constitutive activation of Notch signaling impairs GI organogenesis and causes defective stomachs in mouse (Kim et al., 2011). We first observed that expression of the Notch-responsive gene *Hairy2* was high in the mesenchyme of the stomach at E4, whereas its expression is undetectable at E7.5 (supplementary material Fig. S2). Interestingly, we found that the expression of both *Hairy1 and Hairy2* was higher in vENCC-ablated stomachs than in the controls (Fig. 4A,C), suggesting that Notch signaling activity is sustained. We then used the avian replication-competent retroviral misexpression system to maintain Notch activity through the expression of Notch1 intracellular domain (NICD), the protein fragment that is released in the cytosol as a constitutively active isoform (Schroeter et al., 1998; Shih and Holland, 2006). Efficient activation of the Notch pathway following NICD misexpression was demonstrated by the ectopic induction of *Hairy2* (Fig. 5F). Specific misexpression of NICD in the developing stomach mesenchyme (Moniot et al., 2004; de Santa Barbara et al., 2005; Notarnicola et al., 2012; supplementary material Fig. S3) induced minor morphological defects (thin stomach) (Fig. 5A) and strongly inhibited smooth muscle development, as demonstrated by the reduction in the expression of smooth muscle markers (αSMA, *Sm22* and myocardin) (Fig. 5B,C,F). Moreover, although NICD-misexpressing stomachs did not present an alteration in *Barx1* expression (Fig. 5D), they demonstrated ectopic expression of markers of intestinal mesenchyme (*Nkx2.3*, *Lef1*) and epithelium (SOX9 and *CdxA*), suggesting that these stomachs also have intestinal features (Fig. 5D,E). Interestingly, we observed the ectopic expression of *Bmp4* in the mesenchyme of NICD-misexpressing stomachs (Fig. 5F). Moreover, we found that the rate of mesenchymal cell death was not drastically affected in NICD-misexpressing stomachs compared with controls, whereas cell proliferation was strongly altered (supplementary material Fig. S5). In summary, sustained Notch signaling activity in the developing stomach phenocopied the defects observed in vENCC-ablated stomachs.

A crucial number of vENCCs is required to maintain stomach identity and differentiation by inhibiting Notch signaling

In order to investigate the requirement of vENCCs in maintaining stomach identity, we set up an organ culture approach to chemically ablate the vENCCs from stomachs dissected at E6.5, once vENCC colonization, GI regionalization and SMC differentiation have been established (supplementary material Fig. S6A). Previous studies described animal models of aganglionosis that can be obtained by treating the GI tract *in vivo* with benzalkonium chloride (BC), a surfactant that selectively removes enteric nerve plexuses (Sato et al., 1978; Sakata et al., 1979; Fox and Bass, 1984; Yoneda et al., 2002; Liu et al., 2013a; Shu et al., 2013) without harming smooth muscle tissues (Sato et al., 1978). We then placed GI tracts in 0.04% BC-containing solution for 10 min, washed several times and cultured them in BC-free solution for 36 h before analyses (Fig. 6A). As control experiments, we show that BC treatment do not have a direct effect on either mesenchyme differentiation, as demonstrated by the normal expression of *Sm22* in blood vessels (supplementary material Fig. S6B), or on the epithelium, as visualized by the comparable expression of *Shh* in control and BC-treated stomachs (Fig. 6E; supplementary material Fig. S6C). Immunofluorescence analysis on stomach sections using anti-HNK-1 and anti-cleaved caspase 3 antibodies showed that at the concentration used, BC specifically induced the apoptosis of vENCCs without any significant effect on mesenchymal cells (Fig. 6C). This was associated with a strong decrease in *Sox10* expression, as demonstrated both by *in situ* hybridization and RT-qPCR analyses (Fig. 6B,E). The expression of stomach mesenchyme marker *Barx1* was unaffected (Fig. 6B,E; supplementary material Fig. S2), confirming the integrity of the mesenchyme upon BC treatment. However, we observed a strong reduction in the expression of smooth muscle markers αSMA, *Sm22* and myocardin in BC-treated stomachs compared with controls, demonstrating smooth muscle dedifferentiation (Fig. 6B,C,E). Moreover, BC treatment of E6.5 stomachs resulted in a strong upregulation of intestinal mesenchyme markers *Nkx2.3*, *Lef1* and *Bmp4* (Fig. 6D,E). Interestingly, we observed a strong upregulation of *Hairy2* expression in BC-treated stomachs compared with controls (Fig. 6D,E), indicating ectopic Notch signaling activity. We hypothesized that vENCCs could regulate stomach identity in part through the control of Notch activity. To examine this possibility, we then placed GI tracts in 0.04% BC-containing solution for 10 min, washed several times and cultured for 36 h at 37°C in BC-free solution in the presence DAPT (Fig. 7A). DAPT is a small cell-permeant molecule that inhibits γ-secretase activity, leading to the blockage of Notch signaling (Geling et al., 2002) and the efficient inhibition of *Hairy2* expression in the intestinal mesenchyme (supplementary material Fig. S7). When BC-treated E6.5 stomachs were cultured in the presence of DAPT, they retained smooth muscle *Sm22* expression and showed normal *Nkx2.3* and *Lef1* expression patterns, in contrast to stomachs exposed only to BC (Fig. 7B). Altogether, these results are in line with a contribution of vENCCs in maintaining stomach mesenchyme identity and differentiation in part through the inhibition of the Notch signaling pathway.

DISCUSSION

Altogether, our findings reveal an unexpected new function of vENCCs during GI tract development in regulating both for establishment and the maintenance of stomach patterning and differentiation. We found that reducing the number of vENCCs impairs stomach development. vENCC-ablated stomachs harbor a thinner mesenchymal layer and ectopically express *Bmp4* and two Notch pathway responsive genes, *Hairy1* and *Hairy2*, suggesting that both BMP and Notch signaling pathways are active in vENCC-ablated stomachs. Previous studies have shown that misexpression of *Bmp4* leads to thinner stomach mesenchyme, diminishes cell proliferation and increases cell apoptosis (Smith et al., 2000), while maintaining Notch signaling during mouse gut development has been shown to induce apoptosis of mesenchymal progenitors (Kim et al., 2011). In our experiments, we did not detect massive apoptosis in NICD-misexpressing and vENCC-ablated stomachs, but rather observed a strong decrease in the rate of cell proliferation. We show that reducing the number of vENCCs induces sustained activation of the BMP and Notch pathways in the stomach mesenchyme, decreases the number of mesenchymal progenitors and impairs stomach smooth muscle development. Previous studies have shown that activation of BMP or sustained Notch signaling activity in the mesenchyme of the stomach impairs smooth muscle development, presumably by limiting the expansion of a pool of mesenchymal progenitors (Smith et al., 2000; Kim et al., 2011). We confirm that both pathways have to be repressed for proper stomach mesenchyme differentiation to take place and additionally show that ectopic Notch activation in the mesenchyme of the stomach induces *Bmp4* expression, suggesting that the Notch pathway is upstream of the BMP pathway. Altogether, this suggests that during their migration in the stomach, vENCCs contribute, through the inhibition of the Notch signaling pathway, to expand a pool of mesenchymal progenitors crucial for the initiation of differentiation. Previous study has also

Development (2015) 142, 331-342 doi:10.1242/dev.118422

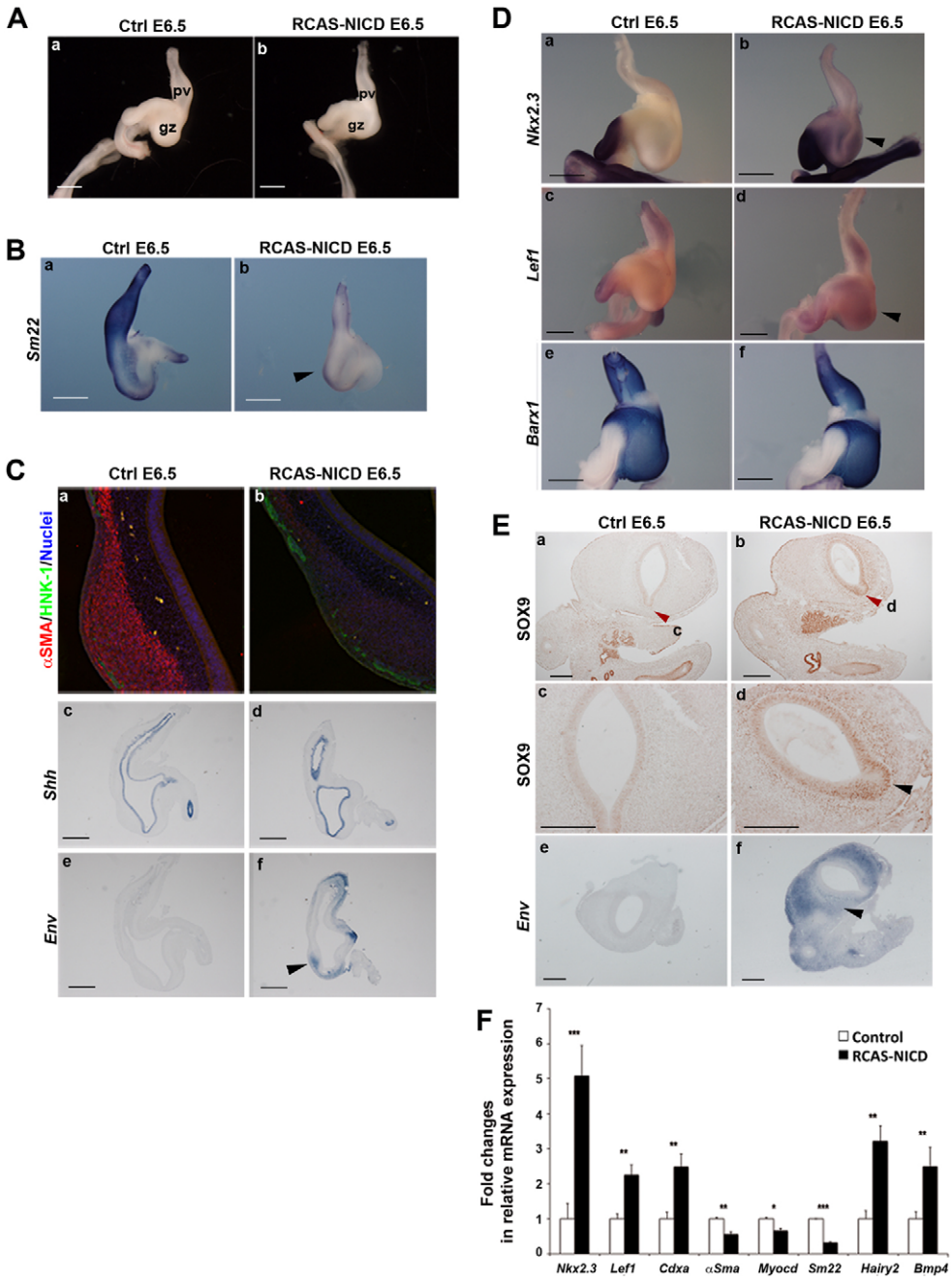

Fig. 5. Notch inhibition is required for stomach patterning and differentiation. Retroviruses expressing control GFP (control) or NICD (RCAS-NICD) were injected in the splanchnopleural mesoderm, which will give rise to the stomach mesenchyme, of HH10 chick embryos. Control and NICD-misexpressing stomachs were dissected at E6.5. (A) Control gut (Ctrl E6.5) (a) and NICD-misexpressing gut (RCAS-NICD E6.5) (b) at E6.5. pv, proventriculus; gz, gizzard. Scale bars: 1 mm. (B) Whole-mount *in situ* hybridization analysis using the *Sm22* probe. Control (Ctrl E6.5) (a) and NICD-misexpressing stomachs (RCAS-NICD E6.5) (b). The black arrowhead in b indicates the low level of *Sm22* expression in the mesenchyme of vENCC-ablated stomachs compared with control. Scale bars: 1 mm. (C) Immunostaining analysis of paraffin-embedded sections from control (Ctrl E6.5) (a) and NICD-misexpressing (RCAS-NICD E6.5) stomachs (b) using anti-αSMA (red, SMA marker) and HNK-1 (green, vENCC marker) antibodies. Nuclei were labeled with Hoechst (blue). *In situ* hybridization of paraffin-embedded sections from control (Ctrl E6.5) (c,e) and NICD-misexpressing (RCAS-NICD E6.5) stomachs (d,f) using *Shh* (c,d) and *Env* (e,f) probes. *Env* staining shows retroviral infection in the mesenchyme (black arrow). Sustained activation of the Notch signaling pathway impairs smooth muscle differentiation. Scale bars: 500 µm in Cc-Cf; 200 µm in Ee,Ef. (D) Whole-mount *in situ* hybridization of control (Ctrl E6.5) (a,c,e) and NICD-misexpressing (RCAS-NICD E6.5) (b,d,f) stomachs using *Nkx2.3* (a,b), *Lef1* (c,d) and *Barx1* (e,f) probes. Sustained expression of NICD induces the expression of intestinal markers *Nkx2.3* and *Lef1* in the stomach mesenchyme (black arrowheads in b and d) although it does not affect the expression of *Barx1*. Scale bars: 1 mm. (E) Immunostaining analysis of paraffin-embedded sections from control (Ctrl E6.5) (a,c) and NICD-misexpressing (RCAS-NICD E6.5) stomachs (b,d) using an anti-SOX9 antibody. Scale bars: 200 µm. c and d are magnified views of the areas highlighted by red arrowheads in a and b. Scale bars: 200 µm in a,b; 500 µm in c,d. The black arrowhead in d highlights the expression of SOX9 in the NICD-misexpressing stomach. (e,f) *In situ* hybridization of paraffin-embedded sections of control (Ctrl E6.5) (e) and NICD-misexpressing (RCAS-NICD E6.5) stomachs (f) using the *Env* probe confirms mesenchymal infection by the retroviruses (black arrowhead in f). Scale bars: 200 µm. (F) Quantification of gene expression by RT-qPCR in E6.5 control (Control) and NICD-misexpressing (RCAS-NICD E6.5) stomachs. Normalized expression levels were converted to fold changes. **P*<0.05, ***P*<0.01, ****P*<0.001. Error bars indicate s.e.m.

Development (2015) 142, 331-342 doi:10.1242/dev.118422

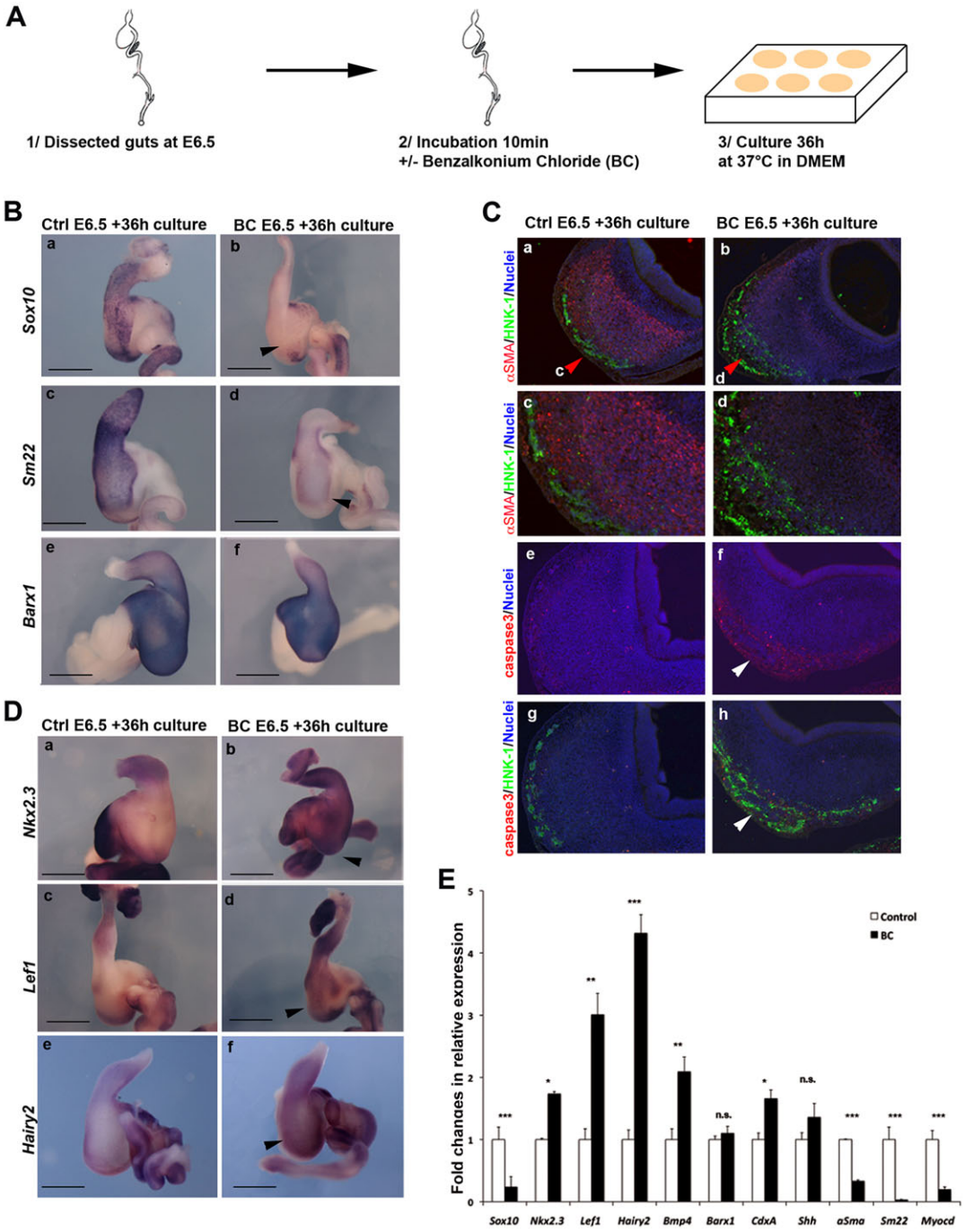

Fig. 6. vENCCs are involved in maintaining stomach identity. (A) Experimental design. Chick guts were dissected at E6.5 and placed in 0.04% BC-containing solution for 10 min, washed several times and cultured in BC-free solution in cell culture dishes at 37°C for 36 h before analyses. (B) Whole-mount *in situ* hybridization of control (Ctrl E6.5+36 h culture) (a,c,e) and BC-treated (BC E6.5+36 h culture) (b,d,f) stomachs with *Sox10* (a,b), *Sm22* (c,d) and *Barx1* (e,f) probes. BC treatment reduces the number of vENCCs (black arrowhead in b) and induces SMC dedifferentiation (black arrowhead in d showing reduction of the *Sm22* signal). The expression of *Barx1* is unchanged upon BC treatment. Scale bars: 1 mm. (C) Immunostaining analysis of paraffin-embedded sections from control (Ctrl E6.5+36 h culture) (a,c,e,g) and BC-treated stomachs (BC E6.5+36 h culture) (b,d,f,h) using anti-αSMA (red; SMC marker) and HNK-1 (green; ENCC marker) antibodies (a-d), or cleaved caspase 3 antibody (e,f) or cleaved caspase 3/HNK-1 antibodies (g,h). c and d are magnified views of the areas indicated by red arrowheads in a and b. White arrowheads in f and g indicate the specific apoptotic effect of BC treatment on vENCCs. (D) Whole-mount *in situ* hybridization of control (Ctrl E6.5+36 h culture) (a,c,e) and BC-treated guts (BC E6.5+36 h culture) (b,d,f) with *Nkx2.3* (a,b), *Lef1* (c,d) and *Hairy2* (e,f) probes. BC-treated stomachs showed elevated expression of *Nkx2.3*, *Lef1* and *Hairy2* in the mesenchyme compared with controls (black arrowheads in b,d,f indicate ectopic gene expression). (E) Quantification of gene expression by RT-qPCR in control (Control) and BC-treated stomachs (BC). Normalized expression levels were converted to fold changes. **P*<0.05, ***P*<0.01, ****P*<0.001, n.s., not significant. Error bars indicate s.e.m.

reported an essential role for neural crest cells in regulating Notch signaling pathways and myogenesis, thus suggesting a general mechanism (Rios et al., 2011).

In this manuscript, we report that a crucial number of vENCCs is necessary for proper patterning of the stomach, thus highlighting an unexpected role for vENCCs in the regionalization of the digestive

Development (2015) 142, 331-342 doi:10.1242/dev.118422

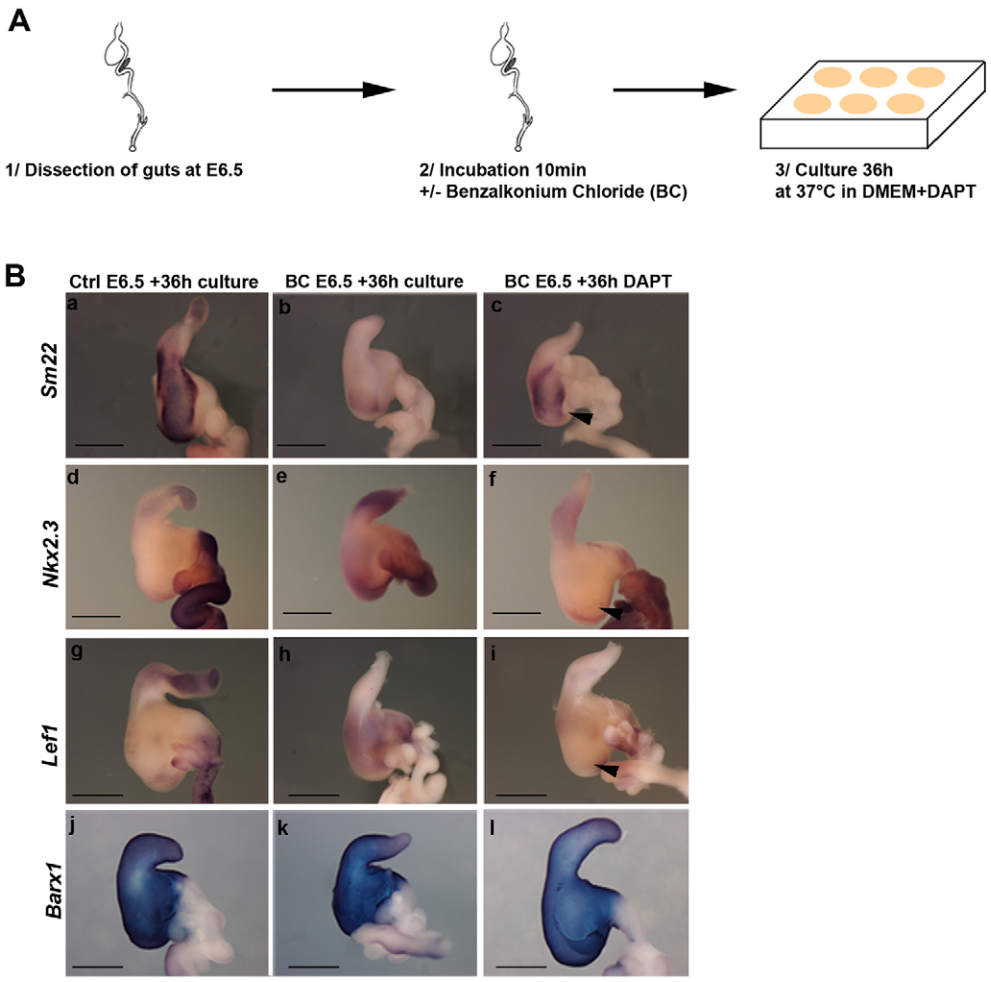

Fig. 7. vENCCs are involved in maintaining stomach identity through inhibition of the Notch signaling pathway. (A) Experimental design. Chick guts were dissected at E6.5 and then placed in 0.04% BC-containing solution for 10 min, washed several times and cultured for 36 h at 37°C in BC-free solution in the presence DAPT. (B) Whole-mount *in situ* hybridization of control (CTRL E6.5+36 h culture) (a,d,g,j), BC-treated (BC E6.5+36 h culture) (b,e,h,k) and BC-treated guts cultured in the presence of DAPT for 36 h (BC E6.5+36 h DAPT) (c,f,i,j) with *Sm22* (a-c), *Nkx2.3* (d-f), *Lef1* (g-i) and *Barx1* (j-l) probes. Scale bars: 1 mm. The inactivation of the Notch pathway upon DAPT treatment restores *Sm22* expression (black arrowhead in c) in BC-treated stomachs. DAPT treatment diminished the expression of intestinal markers *Nkx2.3* and *Lef1* observed following BC treatment (black arrowheads in f and i). *Barx1* expression remains unchanged upon BC and DAPT treatments.

tract along the AP axis and more precisely in stomach identity. Indeed, we observed the expression of intestinal mesenchyme markers in vENCC-ablated stomachs. Moreover, we observed that the identity of gastric epithelium was affected in vENCC-ablated stomachs following the transition from stomach mesenchyme to the mixed stomach/intestine phenotype. However, we cannot exclude that a reduced number of vENCCs directly impacts on the epithelium identity. Altogether, our data reveal that, through the regulation of mesenchyme identity, vENCCs act as a new component in the mesenchymal-epithelial interactions that control proper stomach patterning.

Homeotic Hox genes are crucial regulators of epithelial-mesenchymal interactions involved in vertebrate GI tract patterning along the AP axis (Roberts et al., 1998; de Santa Barbara and Roberts, 2002). Downstream of Hox genes, specific morphogens are involved in this process such as *Bmp4*, which is expressed in the entire GI tract, but not in the stomach. It has been shown that ectopic expression of *Bmp4* in the stomach mesenchyme leads to defects in patterning, as demonstrated by the ectopic expression of the pyloric marker *Nkx2.5*. However, ectopic BMP4 expression does not induce ectopic intestinal markers in the stomach (Smith et al., 2000; S.F., J.M., S.S. and P.d.S.B., unpublished). We observed that Notch signaling is higher in vENCC-ablated stomachs. In line with this observation, we found that constitutive activation of Notch signaling is sufficient to induce intestinal mesenchyme and epithelium markers in the stomach, demonstrating a new role for Notch signaling in regulating the patterning of the GI tract along the AP axis. Interestingly, these results indicate that although both BMP and Notch pathways control the number of mesenchymal progenitors, constitutive Notch activity leads to the acquisition of intestinal mesenchyme and epithelium features, whereas BMP4 misexpression does not, suggesting an additional role for Notch signaling in regulating intestinal development. We show here that inhibition of the Notch pathway in the mesenchyme, through a contribution of vENCCs, is a prerequisite for the establishment of gastric identity, supporting the involvement of specific molecular and tissue interactions for the establishment of gastric features. Altogether, our observations are in line with previous studies demonstrating that intestinal differentiation is a default state of gut endoderm (Kim et al., 2005).

Interestingly, we show that chemical ablation of vENCCs upon BC treatment on patterned and differentiated GI tract leads to the transition of the stomach into a stomach-intestinal mixed phenotype and to the dedifferentiation of the smooth muscle structure, suggesting that a crucial number of vENCCs is required for maintaining stomach identity and differentiation. Smooth muscle plasticity is a mechanism that is common to all smooth muscle cell types (vascular, visceral and digestive) and is activated in response to normal or pathological stimuli, leading to the conversion of contractile and functional smooth muscle cells into undifferentiated, proliferative and migratory cells (Owens et al., 2004). We have previously shown that alteration of BMP and FGF pathway activities in differentiated SMCs induce their dedifferentiation (Le Guen et al., 2009; Notarnicola et al., 2012). Interestingly, we show here

Development (2015) 142, 331-342 doi:10.1242/dev.118422

that both *Bmp4* and *Hairy2* are ectopically expressed in the mesenchyme of BC-treated stomachs, suggesting that the activation of Notch, in addition to the BMP pathway regulate SMC plasticity. In addition, we report that vENCCs participate in maintenance of stomach identity and differentiation through inhibition of the Notch signaling pathway. These complementary data suggest that the molecular mechanisms regulated by vENCCs are comparable in both the establishment and maintenance of stomach identity.

Understanding in molecular terms how vENCCs regulate Notch activity would be interesting. vENCCs could regulate Notch pathway activity through a direct mechanism. Testing this hypothesis would involve first analyzing the expression pattern of Notch genes and receptors. The mammalian Notch genes encode for a family of four transmembrane receptors and their multiple Delta and Jagged ligands. It has been shown in mouse that Notch1, Delta1, Delta3 and Jagged2 are expressed in ENCCs, whereas both Notch1 and Notch3 are present in the gut mesenchyme and Notch2 is not detected in ENCCs (Okamura and Saga, 2008; Kim et al., 2011). In summary, Notch ligands and receptors are expressed in the developing stomach in both the mesenchyme and the vENCCs, making it challenging to address whether vENCCs regulate Notch activity through a direct mechanism.

Moreover, this would not exclude that vENCCs could regulate Notch activity in the mesenchyme through indirect molecular mechanisms, as ENCCs secrete numerous ligands and their receptors are expressed in the mesenchyme. Interestingly, ENCCs secrete WNT ligands (Serralbo and Marcelle, 2014) and WNT signaling is essential for stomach development (Theodosiou and Tabin, 2003). Furthermore, it has been shown that WNT signaling limits Notch activity in cell culture (Collu et al., 2012; Liu et al., 2013b), supporting the idea that WNT ligands secreted from vENCCs could activate WNT signaling in the mesenchyme, which in turn could lead to the inhibition of Notch activity. Testing this hypothesis would first imply an analysis of the expression of multiple WNT ligands in our system to determine which one(s) is (are) expressed in the vENCCs in order to examine to what extent the modulation of WNT activity specifically in the mesenchyme affects both stomach patterning/differentiation and Notch activity. In addition, ENCCs are known to secrete other morphogens, such as BMP and FGF, and all of these signaling pathways could also be involved in the regulation of Notch activity and would also need to be tested.

As previously commented, epithelial-mesenchymal interactions are essential for the development and differentiation of the GI tract. Studies have demonstrated that endodermal Hh signaling is required for both the patterning and differentiation of the gut mesenchyme (Ramalho-Santos et al., 2000; Sukegawa et al., 2000; Reichenbach et al., 2008; Mao et al., 2010; Liu and Ngan, 2014), presumably through the regulation of the Notch signaling activity (Kim et al., 2011). In this study, we show that vENCCs participate in stomach patterning and differentiation through the regulation of Notch activity. Interestingly, it has been shown that endodermal Hh signaling regulates ENS development (Ramalho-Santos et al., 2000; Sukegawa et al., 2000; Reichenbach et al., 2008; Mao et al., 2010; Liu and Ngan, 2014). Accordingly, vENCCs express the Hh receptor Patched and Hh signaling specifically regulates their proliferation, migration and differentiation (Fu et al., 2004; Reichenbach et al., 2008). We could thus speculate that Hh plays several roles in Notch signaling and GI tract development through the regulation of ENS development. Altogether, our data reveal that vENCCs could act as a new mediator in the mesenchymal-epithelial interactions that control stomach development.

MATERIALS AND METHODS

Retroviral misexpression system and *in ovo* microsurgery

Fertilized white Leghorn chicken eggs (Haas Farm, France) were incubated at 38°C in a humidified incubator (Coudelou, France) until use. Embryos were staged by according to Hamburger and Hamilton (HH) (Hamburger and Hamilton, 1951). Gastrointestinal (GI) tissues were dissected and staged by embryonic day (E) (Southwell, 2006). The RCAS vector to produce replication-competent retroviruses (RCAS) has been previously described (Moniot et al., 2004; Le Guen et al., 2009). The DF-1 chicken fibroblast cell line (ATCC-LGC) was transfected with RCAS-based constructs to produce retroviruses expressing GFP alone (Moniot et al., 2004), NICD (Shih and Holland, 2006) or BMP4 (Smith et al., 2000). Retroviruses were injected in the splanchnopleural mesoderm of HH10 chick embryos to target the stomach mesenchyme (Roberts et al., 1998; Moniot et al., 2004; Le Guen et al., 2009; Notarnicola et al., 2012). Eggs were then placed at 38°C until harvested. Ablation of vENCCs was performed by microsurgically removing the neural tube and associated neural crest between somites 3 and 6 in HH9 to HH11 chick embryos, as previously described (Burns et al., 2000; Barlow et al., 2008). In our experiments, the survival rate was 21% (n=120/590).

Gastrointestinal organ cultures

Chick E6.5 GI tracts were freshly dissected and used for organ cultures. Organs were cultured in Dulbecco's modified Eagle medium (DMEM) in presence of 0.2% BSA and 5 µg/ml insulin in uncoated dishes for 36 h. The optimal concentration of each compound was determined by evaluating the effects on *Sox10* and *Sm22* expression of different concentrations (supplementary material Fig. S6). Incubation with 0.04% BC solution (Sigma) was carried out at room temperature for 10 min. InSolution γ-Secretase Inhibitor IX (DAPT) [Calbiochem; 50 µM dissolved in DMSO; (Daudet et al., 2007)] was added to the medium for 36 h and compared with controls.

In situ hybridization and immunofluorescence staining

For whole-mount *in situ* hybridization, dissected GI tissues were fixed in 4% paraformaldehyde at room temperature for 1 h, washed in PBS, gradually dehydrated in methanol and stored at −20°C before processing for whole-mount *in situ* hybridization as described previously (Moniot et al., 2004; Le Guen et al., 2009). For sections, GI tissues were fixed in 4% paraformaldehyde at room temperature for 1 h, washed in PBS, gradually dehydrated in ethanol and embedded in paraffin. Sections (10 µm) were cut using a microtome and collected on poly-L-lysine-coated slides (Thermo Fisher). *In situ* hybridization experiments on paraffin sections were carried out as previously described (Faure et al., 2013). Published chick probes were used: *Barx1* (clone ChEST322m23, ARK Genomics, UK), *Bmp4* (Roberts et al., 1995), *Nkx2.3* (Smith et al., 2000), *Nkx2.5* (Smith et al., 2000), *Bapx1* (Nielsen et al., 2001), *Env* (Le Guen et al., 2009), *Shh* (Roberts et al., 1995), *Sm22* (Faure et al., 2013), *Lef1* (Theodosiou and Tabin, 2003), *Hairy2* (Jouve et al., 2000). Hematoxylin and Eosin (H&E) staining was performed using standard procedures. Immunofluorescence studies were performed on paraffin sections using polyclonal antibodies against αSMA (Sigma) and SOX9 (Chemicon) and monoclonal antibodies against calponin (Sigma), HNK-1 (NeoMarker), TUJ1 (Covance), cleaved caspase 3 (5A1E, Cell Signaling) and phospho-histone H3-Ser10 (PH3) (Millipore). Nuclei were labeled with Hoechst (Invitrogen). Images were acquired using a Nikon-AZ100 stereomicroscope and a Carl-Zeiss AxioImager microscope.

Reverse transcription and quantitative polymerase chain reaction (RT-qPCR)

For vENCC-ablated, NICD misexpression and BC-treated stomach experiments, total RNAs were extracted from five pools of five combined stomachs with the HighPure RNA Isolation kit (Roche), and qPCR was performed using LightCycler technology (Roche Diagnostics). Each sample was analyzed in three independent experiments carried out in triplicate. Expression levels were determined with the LightCycler analysis software (version-3.5) relative to standard curves. Data were represented as the mean level of gene expression relative to the expression of the reference gene *Gapdh* as previously described (Notarnicola et al., 2012). Data were

Development (2015) 142, 331-342 doi:10.1242/dev.118422

analyzed using unpaired Student's *t*-test in GraphPad Prism 5 software and results were considered significant when $*P<0.05$, $**P<0.01$ or $***P<0.001$. PCR primers (supplementary material Table S1) were designed using the LightCycler Probe Design software 2.0.

Acknowledgements

We thank members of INSERM U1046 unit for comments on the work and manuscript. We thank S. Thorsteinsdottir for providing chick *Hairy2* probe and E. Holland for the RCAS-NICD construct.

Competing interests

The authors declare no competing financial interests.

Author contributions

S.F. and P.d.S.B. designed the experiments, obtained findings and wrote the manuscripts. S.F., J.M. and S.S. carried out experiments and analyzed data.

Funding

Research was supported by AFM Trampolin to S.F. and by the French Patients' Association POIC and Fondation ARC to P.d.S.B. J.M. had a French Ministry studentship and S.S. had a University Montpellier 1 post-doctoral fellowship.

Supplementary material

Supplementary material available online at
http://dev.biologists.org/lookup/suppl/doi:10.1242/dev.118422/-/DC1

References

Barlow, A. J., Bogardi, J.-P., Ladher, R. and Francis-West, P. H. (1999). Expression of chick Barx-1 and its differential regulation by FGF-8 and BMP signaling in the maxillary primordia. *Dev. Dyn.* **214**, 291-302.

Barlow, A. J., Wallace, A. S., Thapar, N. and Burns, A. J. (2008). Critical numbers of neural crest cells are required in the pathways from the neural tube to the foregut to ensure complete enteric nervous system formation. *Development* **135**, 1681-1691.

Blache, P., van de Wetering, M., Duluc, I., Domon, C., Berta, P., Freund, J.-N., Clevers, H. and Jay, P. (2004). SOX9 is an intestine crypt transcription factor, is regulated by the Wnt pathway, and represses the CDX2 and MUC2 genes. *J. Cell Biol.* **166**, 37-47.

Buchberger, A., Pabst, O., Brand, T., Seidl, K. and Arnold, H.-H. (1996). Chick NKx-2.3 represents a novel family member of vertebrate homologues to the Drosophila homeobox gene tinman: differential expression of cNKx-2.3 and cNKx-2.5 during heart and gut development. *Mech. Dev.* **56**, 151-163.

Burns, A. J. and Le Douarin, N. M. (1998). The sacral neural crest contributes neurons and glia to the post-umbilical gut: spatiotemporal analysis of the development of the enteric nervous system. *Development* **125**, 4335-4347.

Burns, A. J., Champeval, D. and Le Douarin, N. M. (2000). Sacral neural crest cells colonise aganglionic hindgut in vivo but fail to compensate for lack of enteric ganglia. *Dev. Biol.* **219**, 30-43.

Collu, G. M., Hidalgo-Sastre, A., Acar, A., Bayston, L., Gildea, C., Leverentz, M. K., Mills, C. G., Owens, T. W., Meurette, O., Dorey, K. et al. (2012). Dishevelled limits Notch signalling through inhibition of CSL. *Development* **139**, 4405-4415.

Daudet, N., Ariza-McNaughton, L. and Lewis, J. (2007). Notch signalling is needed to maintain, but not to initiate, the formation of prosensory patches in the chick inner ear. *Development* **134**, 2369-2378.

de Santa Barbara, P. and Roberts, D. J. (2002). Tail gut endoderm and gut/genitourinary/tail development: a new tissue-specific role for Hoxa13. *Development* **129**, 551-561.

de Santa Barbara, P., van den Brink, G. R. and Roberts, D. J. (2002). Molecular etiology of gut malformations and diseases. *Am. J. Med. Genet.* **115**, 221-230.

de Santa Barbara, P., van den Brink, G. R. and Roberts, D. J. (2003). Development and differentiation of the intestinal epithelium. *Cell. Mol. Life Sci.* **60**, 1322-1332.

de Santa Barbara, P., Williams, J., Goldstein, A. M., Doyle, A. M., Nielsen, C., Winfield, S., Faure, S. and Roberts, D. J. (2005). Bone morphogenetic protein signaling pathway plays multiple roles during gastrointestinal tract development. *Dev. Dyn.* **234**, 312-322.

Fairman, C. L., Clagett-Dame, M., Lennon, V. A. and Epstein, M. L. (1995). Appearance of neurons in the developing chick gut. *Dev. Dyn.* **204**, 192-201.

Faure, S. and de Santa Barbara, P. (2011). Molecular embryology of the foregut. *J. Pediatr. Gastroenterol. Nutr.* **52** Suppl. 1, S2-S3.

Faure, S., Georges, M., McKey, J., Sagnol, S. and de Santa Barbara, P. (2013). Expression pattern of the homeotic gene Bapx1 during early chick gastrointestinal tract development. *Gene Expr. Patterns* **13**, 287-292.

Fox, D. A. and Bass, P. (1984). Selective myenteric neuronal denervation of the rat jejunum. Differential control of the propagation of migrating myoelectric complex and basic electric rhythm. *Gastroenterology* **87**, 572-577.

Fu, M., Lui, V. C. H., Sham, M. H., Pachnis, V. and Tam, P. K. H. (2004). Sonic hedgehog regulates the proliferation, differentiation, and migration of enteric neural crest cells in gut. *J. Cell Biol.* **166**, 673-684.

Furness, J. B. (2006). The organisation of the autonomic nervous system: peripheral connections. *Auton. Neurosci.* **130**, 1-5.

Gabella, G. (2002). Development of visceral smooth muscle. *Results Probl. Cell Differ.* **38**, 1-37.

Geling, A., Steiner, H., Willem, M., Bally-Cuif, L. and Haass, C. (2002). A gamma-secretase inhibitor blocks Notch signaling in vivo and causes a severe neurogenic phenotype in zebrafish. *EMBO Rep.* **3**, 688-694.

Hamburger, V. and Hamilton, H. L. (1951). A series of normal stages in the development of the chick embryo. *J. Morphol.* **88**, 49-92.

Jouve, C., Palmeirim, I., Henrique, D., Beckers, J., Gossler, A., Ish-Horowicz, D. and Pourquié, O. (2000). Notch signalling is required for cyclic expression of the hairy-like gene HES1 in the presomitic mesoderm. *Development* **127**, 1421-1429.

Kedinger, M., Simon-Assmann, P. M., Lacroix, B., Marxer, A., Hauri, H. P. and Haffen, K. (1986). Fetal gut mesenchyme induces differentiation of cultured intestinal endodermal and crypt cells. *Dev. Biol.* **113**, 474-483.

Kedinger, M., Simon-Assmann, P., Bouziges, F., Arnold, C., Alexandre, E. and Haffen, K. (1990). Smooth muscle actin expression during rat gut development and induction in fetal skin fibroblastic cells associated with intestinal embryonic epithelium. *Differentiation* **43**, 87-97.

Kim, B.-M., Buchner, G., Miletich, I., Sharpe, P. T. and Shivdasani, R. A. (2005). The stomach mesenchymal transcription factor Barx1 specifies gastric epithelial identity through inhibition of transient Wnt signaling. *Dev. Cell* **8**, 611-622.

Kim, T.-H., Kim, B.-M., Mao, J., Rowan, S. and Shivdasani, R. A. (2011). Endodermal Hedgehog signals modulate Notch pathway activity in the developing digestive tract mesenchyme. *Development* **138**, 3225-3233.

Kosinski, C., Stange, D. E., Xu, C., Chan, A. S., Ho, C., Yuen, S. T., Mifflin, R. C., Powell, D. W., Clevers, H., Leung, S. Y. et al. (2010). Indian hedgehog regulates intestinal stem cell fate through epithelial-mesenchymal interactions during development. *Gastroenterology* **139**, 893-903.

Le Douarin, N. M. and Teillet, M. A. (1973). The migration of neural crest cells to the wall of the digestive tract in avian embryo. *J. Embryol. Exp. Morphol.* **30**, 31-48.

Le Guen, L., Notarnicola, C. and de Santa Barbara, P. (2009). Intermuscular tendons are essential for the development of vertebrate stomach. *Development* **136**, 791-801.

Liu, J. A.-j. and Ngan, E. S.-W. (2014). Hedgehog and notch signaling in enteric nervous system development. *Neurosignals* **22**, 1-13.

Liu, W., Yue, W. and Wu, R. (2013a). Overexpression of Bcl-2 promotes survival and differentiation of neuroepithelial stem cells after transplantation into rat aganglionic colon. *Stem Cell Res. Ther.* **4**, 7.

Liu, X.-H., Wu, Y., Yao, S., Levine, A. C., Kirschenbaum, A., Collier, L., Bauman, W. A. and Cardozo, C. P. (2013b). Androgens up-regulate transcription of the Notch inhibitor Numb in C2C12 myoblasts via Wnt/β-catenin signaling to T cell factor elements in the Numb promoter. *J. Biol. Chem.* **288**, 17990-17998.

Lorentz, O., Duluc, I., Arcangelis, A. D., Simon-Assmann, P., Kedinger, M. and Freund, J.-N. (1997). Key role of the Cdx2 homeobox gene in extracellular matrix-mediated intestinal cell differentiation. *J. Cell Biol.* **139**, 1553-1565.

Mao, J., Kim, B. M., Rajurkar, M., Shivdasani, R. A. and McMahon, A. P. (2010). Hedgehog signaling controls mesenchymal growth in the developing mammalian digestive tract. *Development* **137**, 1721-1729.

Moniot, B., Biau, S., Faure, S., Nielsen, C. M., Berta, P., Roberts, D. J. and de Santa Barbara, P. (2004). SOX9 specifies the pyloric sphincter epithelium through mesenchymal-epithelial signals. *Development* **131**, 3795-3804.

Nielsen, C., Murtaugh, L. C., Chyung, J. C., Lassar, A. and Roberts, D. J. (2001). Gizzard formation and the role of Bapx1. *Dev. Biol.* **231**, 164-174.

Notarnicola, C., Rouleau, C., Le Guen, L., Virsolvy, A., Richard, S., Faure, S. and De Santa Barbara, P. (2012). The RNA-binding protein RBPMS2 regulates development of gastrointestinal smooth muscle. *Gastroenterology* **143**, 687–697.e9.

Okamura, Y. and Saga, Y. (2008). Notch signaling is required for the maintenance of enteric neural crest progenitors. *Development* **135**, 3555-3565.

Owens, G. K., Kumar, M. S. and Wamhoff, B. R. (2004). Molecular regulation of vascular smooth muscle cell differentiation in development and disease. *Physiol. Rev.* **84**, 767-801.

Peters-van der Sanden, M. J. H., Kirby, M. L., Gittenberger-de Groot, A., Tibboel, D., Mulder, M. P. and Meijers, C. (1993). Ablation of various regions within the avian vagal neural crest has differential effects on ganglion formation in the fore-, mid- and hindgut. *Dev. Dyn.* **196**, 183-194.

Ramalho-Santos, M., Melton, D. A. and McMahon, A. P. (2000). Hedgehog signals regulate multiple aspects of gastrointestinal development. *Development* **127**, 2763-2772.

Reichenbach, B., Delalande, J.-M., Kolmogorova, E., Prier, A., Nguyen, T., Smith, C. M., Holzschuh, J. and Shepherd, I. T. (2008). Endoderm-derived Sonic hedgehog and mesoderm Hand2 expression are required for enteric nervous system development in zebrafish. *Dev. Biol.* **318**, 52-64.

Development (2015) 142, 331-342 doi:10.1242/dev.118422

Rios, A. C., Serralbo, O., Salgado, D. and Marcelle, C. (2011). Neural crest regulates myogenesis through the transient activation of NOTCH. *Nature* **473**, 532-535.
Roberts, D. J. (2000). Molecular mechanisms of development of the gastrointestinal tract. *Dev. Dyn.* **219**, 109-120.
Roberts, D. J., Johnson, R. L., Burke, A. C., Nelson, C. E., Morgan, B. A. and Tabin, C. J. (1995). Sonic hedgehog is an endodermal signal inducing Bmp-4 and Hox genes during induction and regionalization of the chick hindgut. *Development* **121**, 3163-3174.
Roberts, D. J., Smith, D. M., Goff, D. J. and Tabin, C. J. (1998). Epithelial-mesenchymal signaling during the regionalization of the chick gut. *Development* **125**, 2791-2801.
Sakata, K., Kunieda, T., Furuta, T. and Sato, A. (1979). Selective destruction of intestinal nervous elements by local application of benzalkonium solution in the rat. *Experientia* **35**, 1611-1613.
Sato, A., Yamamoto, M., Imamura, K., Kashiki, Y., Kunieda, T. and Sakata, K. (1978). Pathophysiology of aganglionic colon and anorectum: an experimental study on aganglionosis produced by a new method in the rat. *J. Pediatr. Surg.* **13**, 399-405.
Schroeter, E. H., Kisslinger, J. A. and Kopan, R. (1998). Notch-1 signalling requires ligand-induced proteolytic release of intracellular domain. *Nature* **393**, 382-386.
Serralbo, O. and Marcelle, C. (2014). Migrating cells mediate long-range WNT signaling. *Development* **141**, 2057-2063.
Shih, A. H. and Holland, E. C. (2006). Notch signaling enhances nestin expression in gliomas. *Neoplasia* **8**, 1072-1082.
Shu, X., Meng, Q., Jin, H., Chen, J., Xiao, Y., Ji, J., Qin, T. and Wang, G. (2013). Treatment of aganglionic megacolon mice via neural stem cell transplantation. *Mol. Neurobiol.* **48**, 429-437.
Silberg, D. G., Swain, G. P., Suh, E. R. and Traber, P. G. (2000). Cdx1 and cdx2 expression during intestinal development. *Gastroenterology* **119**, 961-971.
Smith, D. M. and Tabin, C. J. (1999). Developmental biology: BMP signalling specifies the pyloric sphincter. *Nature* **402**, 748-749.
Smith, D. M., Nielsen, C., Tabin, C. J. and Roberts, D. J. (2000). Roles of BMP signaling and Nkx2.5 in patterning at the chick midgut-foregut boundary. *Development* **127**, 3671-3681.
Southwell, B. R. (2006). Staging of intestinal development in the chick embryo. *Anat. Rec. A Discov. Mol. Cell. Evol. Biol.* **288A**, 909-920.
Sukegawa, A., Narita, T., Kameda, T., Saitoh, K., Nohno, T., Iba, H., Yasugi, S. and Fukuda, K. (2000). The concentric structure of the developing gut is regulated by Sonic hedgehog derived from endodermal epithelium. *Development* **127**, 1971-1980.
Theodosiou, N. A. and Tabin, C. J. (2003). Wnt signaling during development of the gastrointestinal tract. *Dev. Biol.* **259**, 258-271.
Tucker, G. C., Aoyama, H., Lipinski, M., Tursz, T. and Thiery, J. P. (1984). Identical reactivity of monoclonal antibodies HNK-1 and NC-1: conservation in vertebrates on cells derived from the neural primordium and on some leukocytes. *Cell Differ.* **14**, 223-230.
Verzi, M. P., Stanfel, M. N., Moses, K. A., Kim, B.-M., Zhang, Y., Schwartz, R. J., Shivdasani, R. A. and Zimmer, W. E. (2009). Role of the homeodomain transcription factor Bapx1 in mouse distal stomach development. *Gastroenterology* **136**, 1701-1710.
Yntema, C. L. and Hammond, W. S. (1954). The origin of intrinsic ganglia of trunk viscera from vagal neural crest in the chick embryo. *J. Comp. Neurol.* **101**, 515-541.
Yoneda, A., Shima, H., Nemeth, L., Oue, T. and Puri, P. (2002). Selective chemical ablation of the enteric plexus in mice. *Pediatr. Surg. Int.* **18**, 234-237.

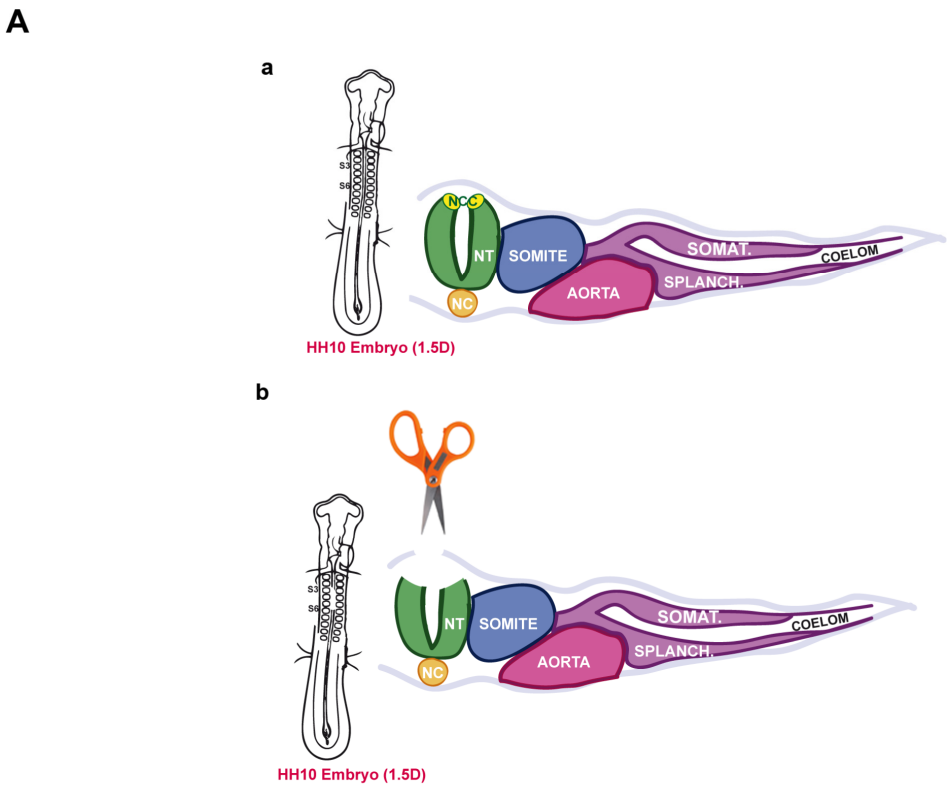

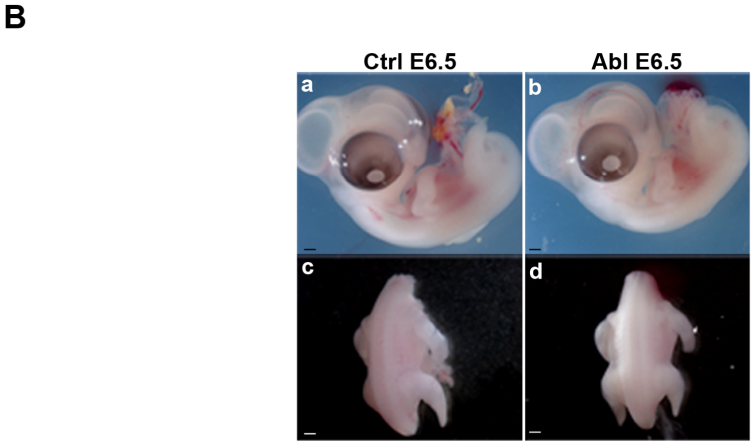

Fig. S1. Ablation of vENCCs in chick embryos. (A) Experimental design. *In ovo* ablation of the dorsal part of the neural tube between somites 3 and 6 where the neural crest cells that will colonize the GI tract are located in HH10 chicken embryos. (a) before and (b) after ablation. Abbreviations: NCC, neural crest cells; Nt, neural tube; NC, notochord; somat, somatopleura; splanch, splanchnopleura. (B) E6.5 control (Ctrl E6.5) (a,c) and vENCC-ablated embryo (Abl E6.5) (b,d). a and b: lateral views; c and d: dorsal views. Scale bars, 1mm.

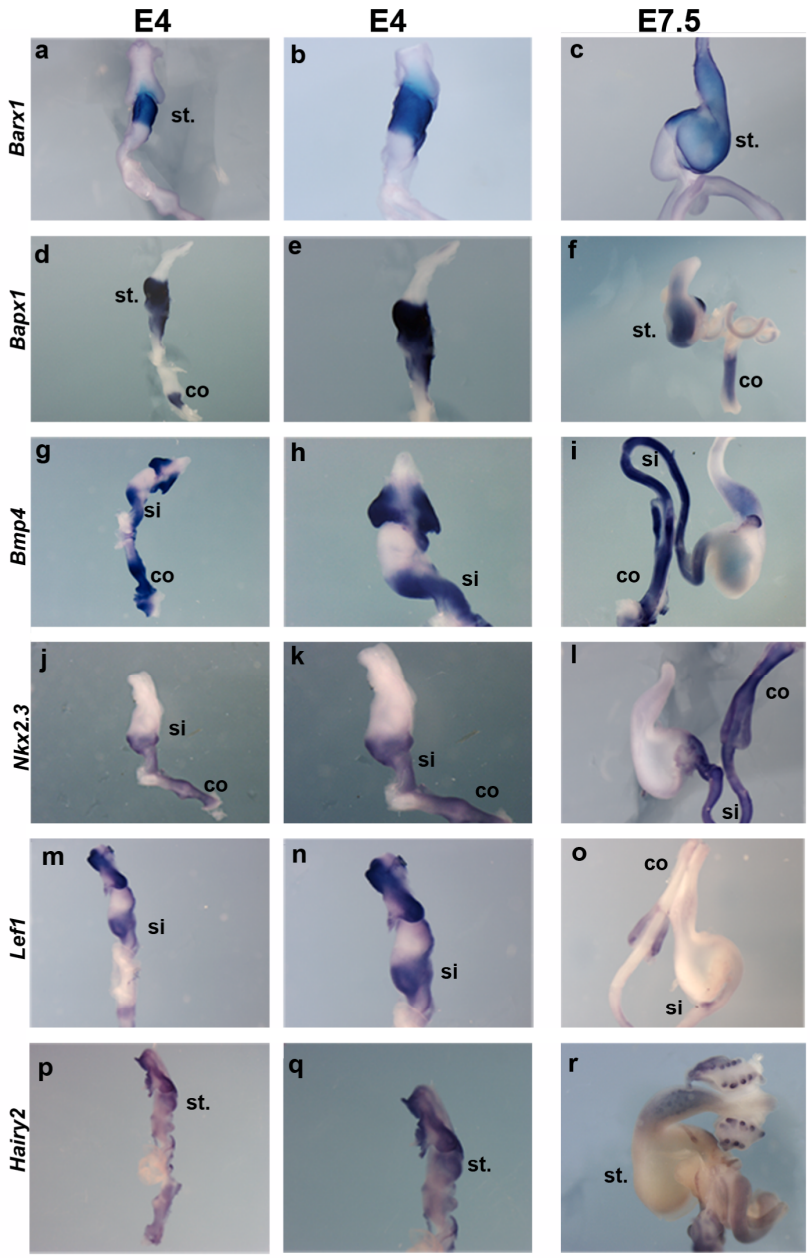

Fig. S2. Expression of *Barx1*, *Bapx1, Bmp4*,, *Nkx2.3, Lef1* and *Hairy2* in the gastrointestinal tract of chick embryos. Whole mount *in situ* hybridization analysis of E4 (a,b,d,e,g,h,j,k,m,n,p,q) and E7.5 (c,f,i,l,o,r) guts using the *Barx1* (a,b,c), *Bapx1* (d,e,f), *Bmp4* (g,h,i) *Nkx2.3* (j,k,l), *Lef1* (m,n,o) and *Hairy2* (p,q,r) probes. Abbreviations: st, stomach; si, small intestine; co, colon.

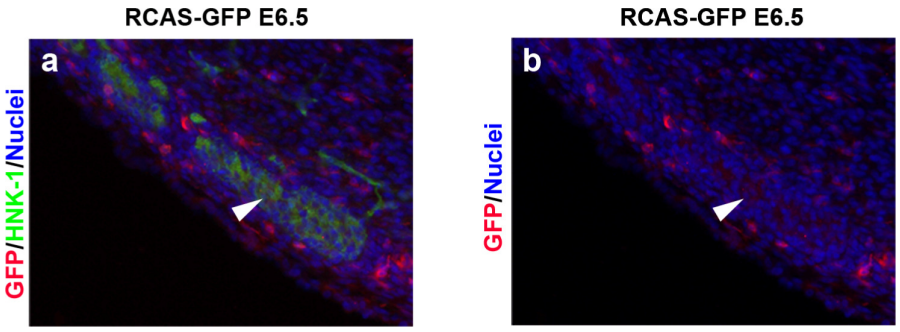

Fig. S3. Efficiency and trophism of avian RCAS retroviruses. Retroviruses expressing GFP were injected in the splanchnopleural mesoderm, which will give rise to the mesenchyme of HH10 embryos. Infected-stomachs (RCAS-GFP E6.5) were fixed at E6.5. Paraffin-embedded stomach sections were analysed by immunofluorescence using anti-GFP (red) and anti-HNK-1 (green) antibodies to specifically detect vENCCs. Nuclei were stained with Hoechst (blue). White arrowheads in a and b show that the HNK-1-positive cells do not express the GFP protein while the mesenchyme does, indicating that GFP retroviruses specifically target the mesenchyme but not the vENCCs.

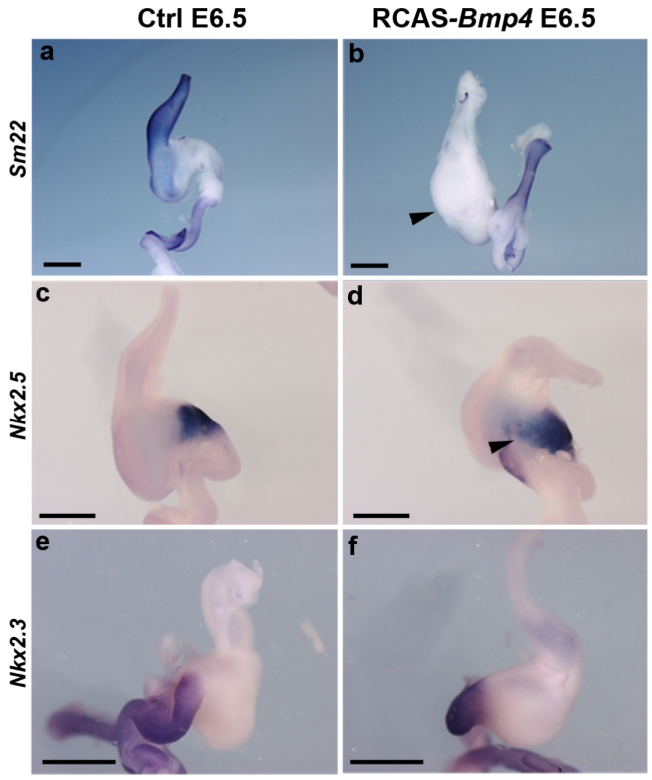

Fig. S4. Impact of *Bmp4* misexpression in the chick developing stomach. Retroviruses expressing GFP (Ctrl) or BMP4 (RCAS-*Bmp4*) were injected in the splanchnopleural mesoderm, which will give rise to the mesenchyme, of HH10 embryos. Control (CTRL E6.5) (a,c,e) and BMP4-overexpressing (RCAS-*Bmp4* E6.5) (b,d,f) guts were dissected at E6.5. Whole mount *in situ* hybridization shows that sustained BMP4 expression impairs *Sm22* expression (as shown by the black arrowhead in b) and promotes *Nkx2.5* expression (black arrowhead in d), but does not affect the expression of *Nkx2.3* (e,f). Scale bars, 1mm.

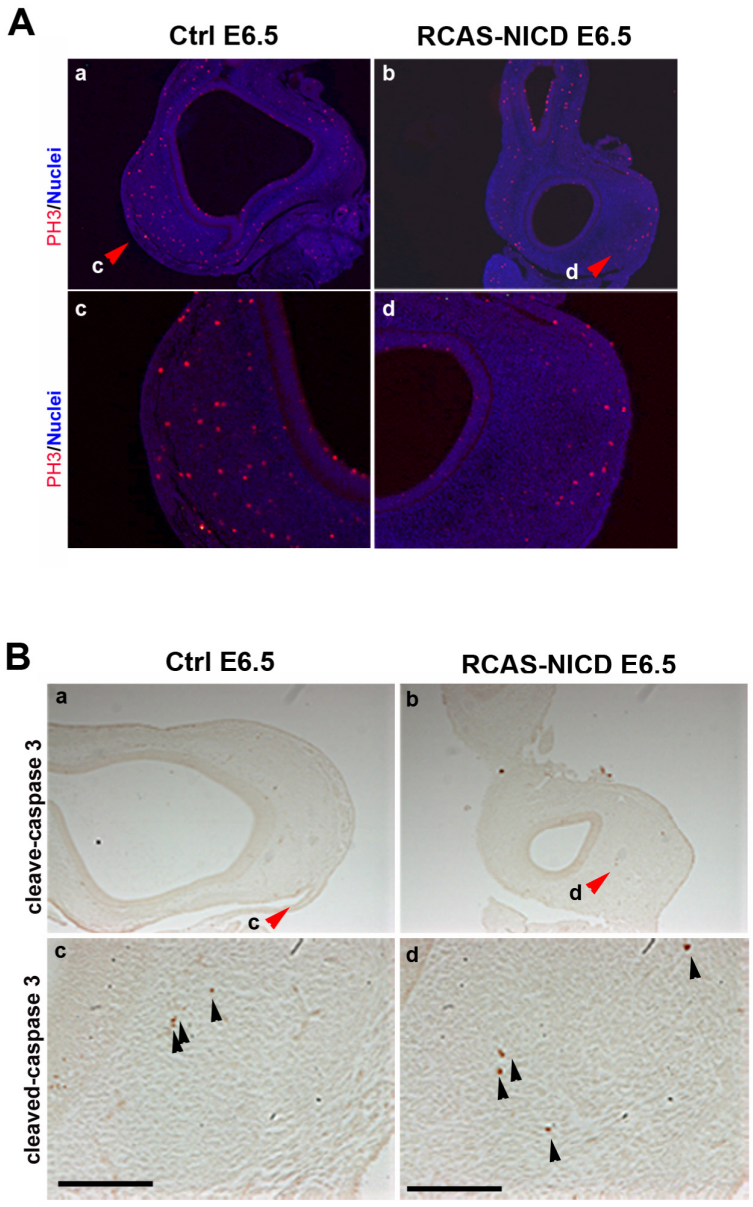

Fig. S5. Impact of NICD missexpression on mesenchymal cell proliferation and apoptosis. Retroviruses expressing control GFP (Ctrl) or NICD (RCAS-NICD E6.5) were injected in the splanchnopleural mesoderm, which will give rise to the stomach mesenchyme, of St.10 chick embryos. Control and NICD-misexpressing stomachs were dissected at E6.5. (A) Immunostaining analysis of paraffin-embedded stomach sections from (a,c) control (Ctrl E6.5) and (b,d) and NICD-misexpressing stomachs (RCAS-NICD E6.5) using anti-PH3 antibody (red; G2/M transition marker). Nuclei were labeled with Hoechst (blue); c and d are

magnified views of the regions indicated by the red arrowheads in a and b. Immunochemistry analysis of paraffin-embedded stomach sections from (a,c) control (Ctrl E6.5) and (b,d) and NICD-misexpressing stomachs (RCAS-NICD E6.5) using anti-cleaved-caspase3 antibody. c and d are magnified views of the regions indicated by red arrowheads in a and b. Black arrowheads point to cleaved-caspase 3-positive apoptotic cells. Scale bars, 100μm.

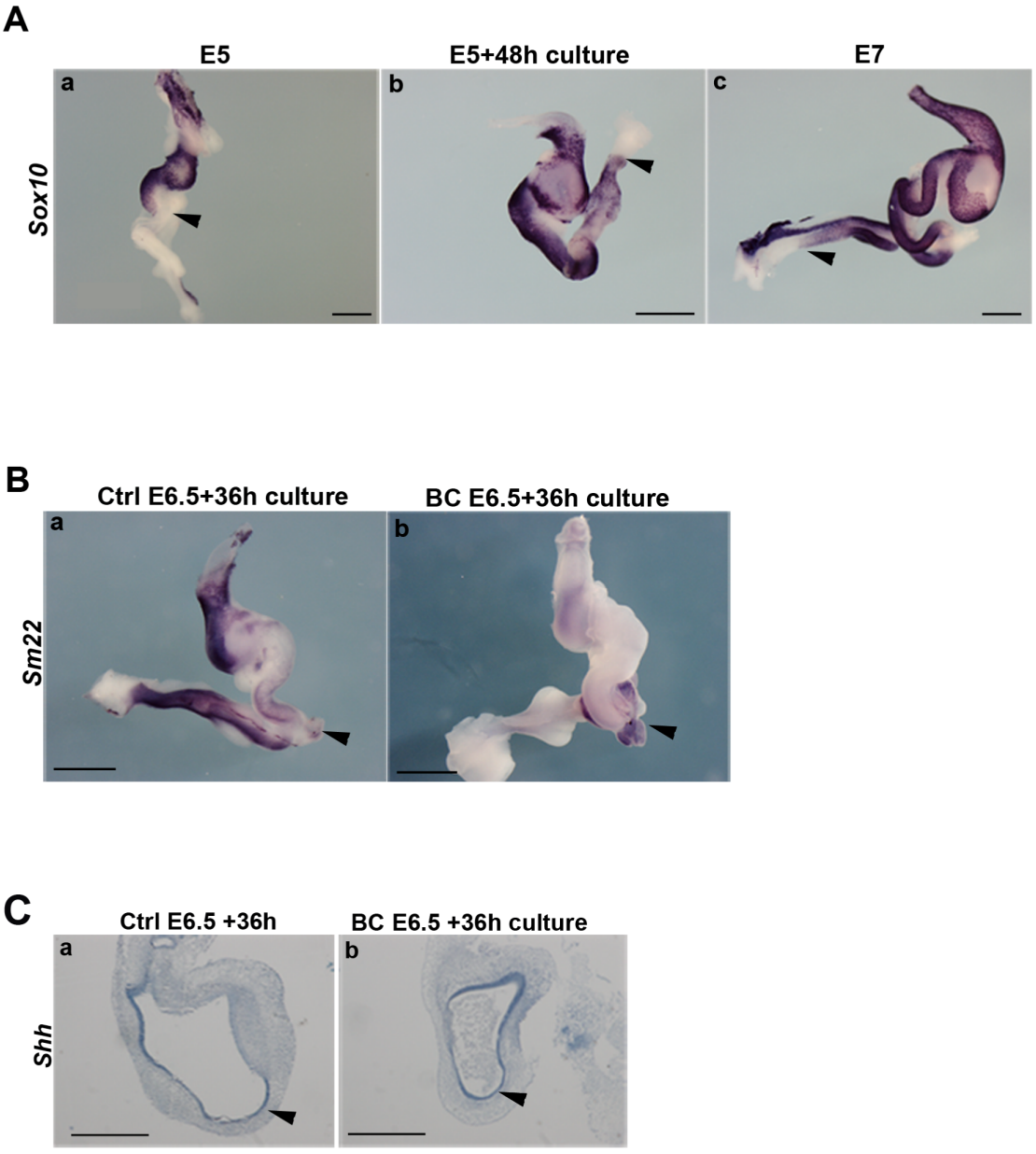

Fig. S6. Control experiments in GI organ culture. (A) Chick guts were dissected at E5 (a) and cultured in cell culture medium at 37°C for 48 hours (E5+48h culture) (b) or dissected at E7 (c). Whole mount *in situ* hybridization analysis using the *Sox10* probe. At E5, migrating vENCCs are in the duodenum (black arrowhead in a). After 48 hours of in vitro cell culture, vENCCs reached the colon (black arrowhead in b) as in E7 gut (black arrowhead in c). Scale

bars, 1mm. (B) Chick guts were dissected at E6.5, incubated (b) or not (control, a) in a 0.04% solution of Benzalkonium Chloride (BC) for 10 minutes, washed several times in cell culture medium and then cultured in cell culture dishes at 37°C for 36 hours. Whole mount *in situ* hybridization using *Sm22* probe shows that BC does not have a direct effect on SMCs as demonstrated by the comparable expression of *Sm22* in blood vessels of both embryos (black arrowheads in a and b). Scale bars, 1mm. (C) *In situ* hybridization of paraffin-embedded sections of control (a) and BC-treated stomach (b) using the *Shh* probe. Scale bars, 500 μm. BC-treated and control stomachs show comparable levels of *Shh* expression in the epithelium (black arrowheads).

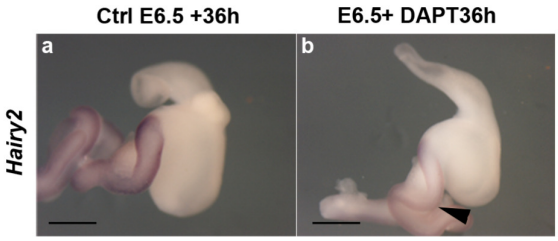

Fig. S7. Gastrointestinal organ culture in the presence of DAPT. Chick guts were dissected at E6.5, incubated or not in a 0.04% solution of Benzalkonium Chloride (BC) for 10 minutes, washed several times in cell culture medium and then incubated at 37°C with DAPT for 36 hours. Chick guts were dissected at E6.5 and cultured in cell culture medium at 37°C for 36 hours in the absence (a) or presence (b) of DAPT. *In situ* hybridization experiment using the *Hairy2* probe. In these conditions, DAPT treatment strongly reduces the expression of the Notch target gene *Hairy2* as indicated by black arrow in b. Scale bars, 1mm.

Table S1. PCR primers used to RT-qPCR analysis.

Targets	Forward primer (5'-3')	Reverse primer (5'-3')	Amplicon (bp)
aSma	CTG TAT GCT TCT GGG CG	GCA GTG GTC ACA AAG GAG	188
Sox10	CCA TCC AGC CAC CAG CA	GAC CCT CAC TCC ATG T	192
Sm22	TGA GCA GGG ATG TCC AGT	AGC CAA TGA TGT TCT TGC C	501
Myocd	CTT CTG TCA GCA ACA CCC	AAG ACT GCG ACT GGT AAC	300
Bmp4	CTT CGT CTT CAA CCT CAG CA	GAC AGC GGC TTC ATC ACT	150
Bapx1	GCA GGT GTT CGA GCT GGA	CTG TCT CTG GTC GTC GC	229
Nkx2.3	ACC TGG AGC ACC ACT TTC A	CGT AGC TGT CGGCAGAG	159
Barx1	CCG CTA CCG CAG TTT CA	GCT CCG CCT TCA GAA CG	152
CdxA	GTC TTC GGT ATT GGT AGC CC	GCT GAG ATT TAT TCT GCT TCG AG	206
Hairy1	CGT CCA ACT GCC TCC TAC	CAG AGC CAG GTG GGA AC	164
Hairy2	GTA CCG CGC CGG CTT CAG	TCA CCA GGG CCT CCA GAC	447
Lef1	AGT CCT CGC TGG TCA AC	CGA TGG TCC CTT GCT GT	174
Shh	CGT AGC TGT CGG CAG AG	TTT CGC TGC CAC TGA GTT T	180
Gapdh	CGT CCT CTC TGG CAA AG	TCA CGC TCC TGG AAG ATA G	177